

Manuscript Number:

Title: Neoproterozoic Re-Os systematics of organic-rich rocks in the São Francisco Basin, Brazil and implications for hydrocarbon exploration

Article Type: Research Paper

Keywords: Re-Os; Neoproterozoic, Canastra; Vazante; Bambuí; source rock

Corresponding Author: Ms. Maria Emilia Bertoni,

Corresponding Author's Institution: Royal Holloway University of London

First Author: Maria Emilia Bertoni

Order of Authors: Maria Emilia Bertoni; Alan D Rooney; David Selby; Fernando F Alkmim; Daniel P Le Heron

Abstract: The São Francisco Basin contains a spectacular archive of Neoproterozoic strata. Its hydrocarbon-bearing strata are receiving increasing attention as global oil and gas exploration targets progressively deeper and older rocks. New Re-Os geochronology for the Paracatú Slate Formation of the Canastra Group, Brazil yields a depositional age of 1002 ± 45 Ma. This age represents the first successful application of the Re-Os system to rocks of this group and indicates excellent agreement with previous published U-Pb detrital zircon age (Rodrigues et al., 2010). Together with TOC values ~ 2 wt.% preserved even after green-schist metamorphism, it might be argued that the São Francisco Basin has had the potential for hydrocarbon generation since Tonian times. We also report an imprecise Re-Os age (1304 ± 210 Ma) for the Serra do Garrote Formation, a further potential source rock of the Vazante Group. We suggest, based on petrological evidence that Re-Os systematics may have been disturbed by post-depositional fluid flow associated with the Vazante hydrothermal alteration. An attempt to determine a Re-Os date for the Sete Lagoas Formation, a putative post-Sturtian cap carbonate, is precluded owing to low Re presence. Major environmental changes in the aftermath of the Jequitaiá glaciation, particularly the development of palaeotopography such as subglacial tunnel valleys, may account for the apparent random distribution of TOC enrichment in these Cryogenian post-glacial deposits. This scenario might thus have major implications for the hydrocarbon prospectivity of this post-glacial succession.

Maria Emilia Bertoni
Department of Earth Sciences
Royal Holloway, University of London
Egham, Surrey, TW20 0EX

London, 20th of November, 2013

Dear Editor,

I am pleased to submit an original research manuscript entitled “*Neoproterozoic Re-Os systematics of organic-rich rocks in the São Francisco Basin, Brazil and implications for hydrocarbon exploration*”. In this article we study three potential source rocks of the São Francisco Basin in order to date them using Re-Os geochronology. The study of Neoproterozoic strata as components of potential petroleum systems is a new and exciting frontier, and one that we feel is entirely appropriate for Precambrian Research. We provide the first depositional isochron for the Canastra Group, and explain the complexities and issues surrounding the application of the technique to other units. We offer a simple model to explain the low TOC values in the Sete Lagoas Formation- a unit representing a cap carbonate above the Sturtian glacial and which was expected to have far higher TOC values than measured. Demonstration of “successful” isochron acquisition is especially important, as in the authors’ experience there has been a general resistance to using this technique in Brazil more generally. The article does not include detailed sedimentological investigations, as the outcrops are almost universally low lying and patchily exposed- and weathered! Thus, samples are limited to cores.

We would suggest the following individuals as potential reviewers: Dr Jonathan Craig (jonathan.craig@eni.com), Dr Robert Creaser (Robert.Creaser@ualberta.ca), Dr Alan Collins (alan.collins@adelaide.edu.au), Dr Sebastian Luening (sebastian.luening@galpenergia.com). We confirm that the manuscript has not been published and is not under consideration for publication elsewhere, and look forward to hearing from you in due course.

Yours sincerely,

Maria Emilia Bertoni

Postgraduate research student
Department of Earth Sciences
Royal Holloway, University of London

- We assess three formations using the rhenium–osmium (Re–Os) geochronometer
- A depositional age of 1002 ± 45 Ma was obtained for the Paracatú Fm.
- Fluid flow is suggested responsible for imprecise ages in the Serra do Garrote Fm.
- Dating of the Sete Lagoas Formation was precluded due to low Rhenium presence
- The São Francisco Basin may have petroleum potential since Tonian times

1 **Neoproterozoic Re-Os systematics of organic-rich rocks in**
2 **the São Francisco Basin, Brazil and implications for**
3 **hydrocarbon exploration**

4
5

6 Maria E. Bertoni^{a,*}, Alan D. Rooney^{b,c}, David Selby^b, Fernando F. Alkmim^d, Daniel
7 P. Le Heron^a

8

9 ^aDepartment of Earth Sciences, Queen's Building, Royal Holloway University of
10 London, Egham, Surrey, TW20 0BY, UK

11 ^bDepartment of Earth Sciences, Durham University, Science Labs, Durham, DH1
12 3LE, United Kingdom.

13 ^cDepartment of Earth and Planetary Sciences, Harvard University, Cambridge, MA,
14 02138, USA

15 ^dDepartamento de Geologia, Escola de Minas, Universidade Federal de Ouro Preto,
16 Morro do Cruzeiro, 35.400.000 Ouro Preto, MG, Brazil

17

18 **Abstract**

19 The São Francisco Basin contains a spectacular archive of Neoproterozoic strata. Its
20 hydrocarbon-bearing strata are receiving increasing attention as global oil and gas
21 exploration targets progressively deeper and older rocks. New Re–Os geochronology
22 for the Paracatú Slate Formation of the Canastra Group, Brazil yields a depositional
23 age of 1002 ± 45 Ma. This age represents the first successful application of the Re–Os
24 system to rocks of this group and indicates excellent agreement with previous
25 published U–Pb detrital zircon age (Rodrigues et al., 2010). Together with TOC
26 values ~ 2 wt.% preserved even after green-schist metamorphism, it might be argued
27 that the São Francisco Basin has had the potential for hydrocarbon generation since
28 Tonian times. We also report an imprecise Re–Os age (1304 ± 210 Ma) for the Serra
29 do Garrote Formation, a further potential source rock of the Vazante Group. We
30 suggest, based on petrological evidence that Re–Os systematics may have been
31 disturbed by post-depositional fluid flow associated with the Vazante hydrothermal
32 alteration. An attempt to determine a Re–Os date for the Sete Lagoas Formation, a
33 putative post-Sturtian cap carbonate, is precluded owing to low Re presence. Major
34 environmental changes in the aftermath of the Jequitaí glaciation, particularly the
35 development of palaeotopography such as subglacial tunnel valleys, may account for
36 the apparent random distribution of TOC enrichment in these Cryogenian post-glacial
37 deposits. This scenario might thus have major implications for the hydrocarbon

38 prospectivity of this post-glacial succession.

39

40 **Keywords:** Re–Os, Neoproterozoic, Canastra, Vazante, Bambuí, source rock

41

42 *Corresponding author. Tel: +44 (0) 1784 443 581. Postal address: Department of
43 Earth Sciences, Royal Holloway University of London, Egham Hill, Egham, Surrey,
44 TW20 0EX, UK. E-mail addresses: maria.bertoni.2009@live.rhul.ac.uk,
45 bertonime@gmail.com. (M. E. Berton)

46

47

48

49 **1.Introduction**

50

51 The rhenium–osmium (Re–Os) geochronometer is an increasingly recognized
52 tool for determining depositional ages of organic-rich rocks (Ravizza and Turekian,
53 1989; Cohen et al., 1999; Selby and Creaser, 2005a; Georgiev et al., 2011) and
54 hydrocarbon deposits (Selby et al, 2005; Selby and Creaser, 2005b). Although the
55 method has yielded absolute dates for Neoproterozoic strata with precision
56 approaching 1% uncertainty (2σ) in units up to greenschist facies (Kendall et al.,
57 2004; Rooney et al., in press), their concordance with those obtained by conventional,
58 geochronological techniques remains controversial in some Proterozoic intervals
59 (Kendall et al., 2006; Kendall et al., 2009a; Mahan et al., 2010).

60

61 In the São Francisco Basin of Brazil (**Fig. 1, A**) the Re–Os radioisotope system
62 has been used to provide Meso-Neoproterozoic depositional ages for the Lapa and
63 Serra do Garrote Formations of the Vazante Group (Geboy, 2006; Azmy et al., 2008).
64 However, the lack of accurate geochronological data throughout the stratigraphy
65 severely hinders attempts to develop a chronological framework for the São Francisco
66 Basin. This is a critical problem for two reasons. First, the São Francisco Basin and its
67 surrounding belts contains a magnificent stratigraphic archive of Proterozoic time,
68 extending at least from the Statherian (1750 Ma) to the Ediacaran (610 Ma) (Alkmim
69 and Martins-Neto, 2012), of wider interest to the Precambrian research community.
70 For example, it exposes, over a wide area, diamictites and associated cap carbonates
71 attributable to Marinoan (Caxito et al., 2012), plus evidence of intra-Cryogenian
72 photosynthetic communities (Olcott et al., 2005). Second, the São Francisco Basin
73 has multiple gas shows, which are probably sourced from Meso-Neoproterozoic
74 organic-rich rocks (Craig et al., 2012 and refs therein). The São Francisco is a frontier
75 basin for hydrocarbon exploration: the origins of these hydrocarbons, the timing of

76 their migration, and mechanism of entrapment, remain unknown. Placing proper
77 geochronological constraints on organic-rich horizons is key to understanding of the
78 nature of the depositional environment and fossil hydrocarbon system in this vast
79 basin.

80

81 The aims of the present paper are threefold: 1) to constrain the depositional
82 age of the organic-rich strata using Re-Os geochronology; 2) to improve radiometric
83 calibration of the Brazilian Proterozoic rock record and contribute to a better
84 understanding of the geological evolution of the Brasília Belt and São Francisco
85 Basin; 3) to establish whether key intervals are enriched in total organic carbon, and
86 hence potential hydrocarbon source rocks. A more detailed sedimentological
87 description of the strata will be presented elsewhere.

88

89 **2. Geological setting and existing chronostratigraphy**

90 The São Francisco craton (**Fig. 1A**), as one of the oldest portions of the Precambrian
91 nucleus of the South American continent, hosts sedimentary successions deposited
92 between the Neoproterozoic (~2800 Ma) and Late Neoproterozoic (580 Ma) (Almeida et
93 al., 2000). Together with other cratons of South America, it represents the internal
94 portions of the plates involved in the assembly of West Gondwana by the end of the
95 Proterozoic Era (Alkmim and Martins-Neto, 2012). The Neoproterozoic Brasiliano-
96 Pan Africano orogenic belts, on the other hand, encompass the margin of those plates
97 and the intervening accretionary material (Alkmim et al., 2001; Alkmim and Martins-
98 Neto, 2012; Almeida et al., 2000). The Brasilia Belt, which flanks the São Francisco
99 Basin to the west, exhibits a fundamentally complex tectonic character and variable
100 metamorphic grade. Therefore, it is essential to briefly outline the structural character,
101 the stratigraphy, and present geochronology of both the Brasília belt and the São
102 Francisco basin.

103

104 "Insert Supplementary Figure 1 here"

105

106 *2.1 The Brasilia Belt and São Francisco basin*

107 The Brasilia Belt, located on the western margin of the São Francisco Craton (**Fig.**
108 **1B**), is the product of a collision between the Amazon, São Francisco-Congo and
109 Paranapanema paleocontinents during the amalgamation of Gondwana (Li et al.,

110 2008; Pimentel et al., 2011; Rodrigues et al., 2012). This belt is composed of thrust
111 sheets verging eastward towards the São Francisco platform (**Fig. 1B**). Metamorphic
112 grade increases progressively westward, reaching granulite facies conditions in the
113 central part of the belt (Dardenne, 2000).

114

115 The southern Brasília Belt, focused in this paper, involves sedimentary rocks
116 grouped into several lithostratigraphic units (**Fig. 1B**): the Araxá, Paranoá, Canastra,
117 and Ibiá groups (Pimentel et al., 2011). Intense deformation, the lack of intercalated
118 volcanics, and the absence of biostratigraphic controls results in multiple possible
119 interpretations for this supracrustal succession (Dardenne, 2000; Valeriano et al.,
120 2008; and references therein). Provenance studies suggest that the Paranoá and
121 Canastra groups are passive margin deposits of the São Francisco paleocontinent,
122 while the Araxá, and Ibiá groups are synorogenic (fore- or back-arc) basin fill
123 (Pimentel et al. 2001; Rodrigues et al. 2010; Pimentel et al., 2011).

124

125 The São Francisco basin occupies the ca. 800 km-long NS-trending lobe of the
126 São Francisco craton (Alkmim and Martins-Neto, 2012) (Fig.1). Bounded to the west
127 and to the east by emergent thrust of the adjacent Brasília and Araçuaí orogenic belts
128 respectively, the basin is filled by Paleo/Mesoproterozoic units (Paranoá Group and
129 Espinhaço Supergroup), and Neoproterzoic strata of the Vazante Group, Jequitaiá
130 Formation, and Bambuí Group (Fig. 1).

131

132 Below, we briefly summarise the characteristics of the Canastra, Vazante and
133 Bambuí groups, as well as the Jequitaiá Formation, which are the focus of the present
134 paper.

135

136 *2.2 Canastra Group*

137 The Canastra Group, mainly present in the southern portion of the eastern Brasília
138 orogen (**Fig. 1B**), comprises phyllite and quartzite with common carbonate beds.
139 These have experienced lower greenschist (chlorite) facies metamorphism (Dardenne,
140 2000). The lithostratigraphy is difficult to unravel owing to numerous thrust faults
141 (Rodrigues et al., 2010) (**Fig. 2**), especially for the basal Serra do Landim Formation
142 (chlorite-rich calc-phyllite and calcschist) and the upper units (Paracatú and the
143 Chapada dos Pilões formations). The Paracatú comprises slope turbidites and basinal,

144 carbonaceous phyllites rich in diagenetic pyrite, whereas the Chapada dos Pilões
145 comprise shallow marine wave and storm-modulated clastics (Pereira et al., 1994).
146 The coarsening upward succession in the upper Canastra Group thus records a
147 regressive, continental platform megasequence (Pereira et al., 1994).

148

149 Pimentel et al., (2001) obtained TDM model ages for Canastra rhythmites
150 from Sm-Nd systematics ranging from 1.9 to 2.3 Ga, suggesting a Paleoproterozoic
151 source from the São Francisco-Congo craton. The youngest detrital zircons are ca.
152 1040 Ma (Valeriano et al., 2004; Rodrigues et al., 2010) (Fig. 2), indicative of a
153 passive margin association within the Brasília Belt (Pimentel et al., 2001, 2011;
154 Rodrigues et al., 2010).—Ore-hosting carbonaceous phyllites of the Morro do Ouro
155 Member of the Paracatú Formation are estimated at 1000 to 1300 Ma, an assumed
156 diagenetic age range based on Rb-Sr, K-Ar chlorite and Pb-Pb on galena (Freitas-
157 Silva, 1996). Metamorphism and gold enrichment of this unit is related to the
158 Brasiliano event at ca. 680 Ma (Freitas-Silva, 1996).

159

160 Thrust contacts characterize the boundaries between the Canastra and lower
161 grade metamorphic strata of the Vazante, Paranoá and Bambuí groups (Pereira et al.,
162 1994). It has been suggested that the Canastra Group is a lateral equivalent of the
163 Paranoá Group (Dardenne, 2000; Pimentel et al., 2011).

164

165 "Insert Supplementary Figure 2 here"

166

167 *2.3 The Vazante Group*

168 The Vazante Group is divided into seven formations (Fig. 3). Broadly, these comprise
169 thick pelitic-dolomitic deposits of marine origin. The formations are metamorphosed
170 to greenschist facies, and are exposed in the eastern Brasília Belt (Fig. 1B).
171 Brasiliano-Pan African thrusts and nappes obscure many sedimentary contacts
172 (Dardenne, 2000), particularly with the Canastra Group to the west and the Bambuí
173 Group to the east (Rodrigues et al., 2012). Intense deformation in the outcrop area in
174 the southern segment of the Brasília belt raises major uncertainties about the internal
175 stratigraphy and lateral correlation of the units.

176

177 In this paper, we analyzed the Serra do Garrote Formation (Fig. 3). This

178 formation is dominantly carbonaceous and pyrite-bearing slate, intercalated with fine
179 quartzite beds, representing an open marine succession deposited below storm wave
180 base (Madalosso, 1980; Madalosso and Valle, 1978). The Serra do Poço Verde lies
181 conformably over the non-carbonate deposits of the Serra do Garrote Formation and is
182 dominantly dolomitic. It also includes slate, carbonaceous phyllite with pyrite and
183 marls (Babinski et al., 2005): glendonite pseudomorphs after ikaite, and dropstones in
184 slates, suggesting paraglacial depositional conditions (Olcott et al., 2005). The Serra
185 do Poço Verde Formation is conformably overlain by the Morro do Calcário
186 Formation – a carbonate-dominated succession including stromatolitic bioherms and
187 biostromes (Dardenne, 2000). This formation is truncated by an unconformity at the
188 base of the overlying Lapa Formation (Misi et al., 2005). The Lapa Formation
189 contains organic-rich shale, which taken together with a $\delta^{13}\text{C}$ negative excursion is
190 interpreted to record the resumption of primary productivity in the aftermath of the
191 Serra de Poço Verde glaciation (Azmy et al., 2006).

192

193 Based on C and Sr isotope curves (Azmy et al., 2006), the Lapa Formation is
194 correlated with the “Sturtian” glacial event (ca. 715 Ma; Macdonald et al., 2010).
195 Globally, the chronometry of the Sturtian glaciation is considered to encompass a ~60
196 Myr window, based on U-Pb zircon and Re-Os geochronology of syn- and postglacial
197 deposits associated with the Rapitan glacials in north western Canada (Macdonald et
198 al., 2010; Rooney et al., in press). Previous Re-Os analyses have yielded depositional
199 ages for organic rich shales of the Serra do Garrote (1353 ± 69 Ma) and Serra do Poço
200 Verde (1126 ± 47 Ma) formations, respectively (Fig. 3; Geboy, 2006). The same
201 technique together with U-Pb measurements on detrital zircons of the Lapa Formation
202 (Azmy et al, 2008) indicated that deposition occurred ca. 1000–1100 Ma. Thus, a late
203 Mesoproterozoic age, rather than a Sturtian assignment, is currently preferred (Azmy
204 et al, 2008). Finally, U–Pb detrital zircon analyses using SHRIMP (Rodrigues et al.,
205 2012) sampled five formations of the Vazante Group. This work identified the
206 youngest population (ca. 930 Ma) at the base of the group, and older populations
207 (ranging ca. 1200–1000 Ma) toward the top (Fig. 3). This suggests either that the
208 Neoproterozoic source was isolated or covered during the evolution of the basin, or
209 that tectonic discontinuities led to tectonic inversion of part of the lithostratigraphic
210 units of the group.

211

212 Despite the complex history of this group, the detrital zircon age pattern of the
213 Serra do Garrote Formation (~1.29 Ga, Rodrigues et al., 2012) is coherent with the
214 isochron Re-Os age (~1.35 Ga, Geboy, 2006) obtained for the same formation.
215 However, the Re-Os isochron (1353 ± 69 Ma) is associated with high MSWD value
216 (26) and the interval of deposition remains quite broad. This raises the possibility that
217 the detrital zircon age is even younger than the Re-Os isochron. Therefore, further
218 provision of radiometric ages is clearly necessary, and motivates our attempts to date
219 the formation.

220

221 "Insert Supplementary Figure 3 here"

222

223 *2.4 Neoproterozoic glacials and the Jequitáí Formation*

224 Evidence for glaciation in the Jequitáí Formation and its correlatives, the Bebedouro
225 Formation and Macaúbas Group, exposed respectively in the northern São Francisco
226 craton and Araçuaí belt (Fig.1), is compelling (e.g. Cukrov et al., 2005; Uhlein et al.,
227 2007; Chaves et al., 2010). The preceding authors have cited a striated pavement cut
228 into the Espinhaço Supergroup in the northeastern portion of the São Francisco basin,
229 together with abundant diamictites with exotic limestones, some of which are well
230 stratified and exhibit unequivocal impact structures implying ice-rafted debris.
231 Furthermore, Martins-Ferreira et al. (2013) describe a ca. 4km-wide valley carved in
232 the sandstones of the Paranoá Group and filled by a package of sandstones,
233 diamictites and tillite of the Jequitáí Formation. These glaciogenic rocks are in turn
234 covered by cap dolomites that mark the base of the Bambuí Group in the western
235 portion of the São Francisco basin. With the exception of the striated pavement, each
236 of these facies are recognised in proprietary cores across the subsurface of the basin.
237 Thus, clear evidence for glacial sedimentary processes at outcrop guides subsurface
238 interpretations.

239 Zircons extracted from the Jequitáí Formation and the correlative Macaúbas
240 Group yielded maximum deposition ages of 880Ma and 864Ma, respectively
241 (Pedrosa-Soares et al., 2000; Rodrigues et al., 2008).

242 Regional seismic sections across the São Francisco Basin (Fig. 4) reveal the
243 presence of major incisions that cut through the top of the Espinhaço II sequence
244 (Alkmim and Martins-Neto, 2012) on the eastern margin of the basin. The dimensions
245 of these valleys range from ~1.5 to ~4 km width and ~100m to ~500 m depth. Their

246 morphology is variable, including forms with flat bottoms and steep sides, and others
247 with a characteristic “v” profile. Almost universally, deformation at the valley
248 margins, in the form of downwarped strata below the incisions, is recognized (**Fig. 4**).
249 Within the valleys, transparent seismofacies are characteristic. The scale of the
250 palaeovalleys is exactly analogous to Sturtian incisions observed elsewhere, such as in
251 Namibia (Le Heron et al., 2012) and in Oman (Van der Vegt et al., 2012).

252

253 Whilst further work is clearly required, we tentatively interpret the
254 palaeovalleys as subglacial tunnel valleys. Their dimensions are analogous to
255 Pleistocene examples of such incisions (Lonergan et al., 2006; Stewart and Lonergan,
256 2011), which are cut under hydrostatically elevated conditions beneath a retreating ice
257 mass. Their dimensions bear a close resemblance to Sturtian examples previously
258 interpreted as such (Le Heron et al., 2012). Furthermore, the downwarped strata at the
259 valley margins are typical of subglacial incisions, with the deformation resulting from
260 ice loading the substrate. The style of fill is presently uncertain, as the palaeovalleys
261 are undrilled, although the seismic transparency of the fill may imply coarse (e.g.
262 diamictite) fill. Assuming a stratigraphic position beneath the Bambuí, it is likely that
263 the incisions are related to the Jequitaí glaciation. Even if the thickness of the
264 Macaúbas Group where the palaeovalleys are imaged (**Fig. 4**) is not compatible with
265 the average thickness of the Jequitaí Formation exposed in adjacent areas (~200 m, F.
266 Alkmim pers. comm.), this unit tends to thinner to the centre of the basin (**Fig. 4**).
267 Therefore, if there were palaeovalleys further inland, these would have been probably
268 infilled with the Jequitaí and basal portion of the Sete Lagoas Formation (as in
269 Martins-Ferreira et al., (2013)). Thus, these incisions are suggested to record the
270 retreat of Jequitaí ice sheets (880 Ma, Rodrigues 2008), which took place during the
271 late rift stage of the Macaúbas basin.

272

273 "Insert Supplementary Figure 4 here"

274

275 *2.5 Bambuí Group*

276 These epicontinental deposits, of alternating siliciclastics and carbonates are the most
277 widely distributed unit in the São Francisco basin (**Fig. 1**), draping the Jequitaí
278 diamictites and sandstones. They form a shallowing upwards sequence (Dardenne,
279 2000; Santos et al., 2000), divisible into three coarsening upward megacycles (**Fig. 5**;

280 Dardenne, 2000) clearly observed in seismic profile in the cratonic area of the São
281 Francisco basin (Martins-Neto, 2009) **Fig. 6**. The first megacycle is represented by
282 the Sete Lagoas Formation, the second includes the Serra de Santa Helena and Lagoa
283 do Jacaré formations and the last cycle comprises the Serra da Saudade and Três
284 Marias formations (Martins and Lemos, 2007).

285

286 "Insert Supplementary Figure 5 here"

287 "Insert Supplementary Figure 6 here"

288

289 The Sete Lagoas Formation, for which we present data in this paper,
290 comprises a succession of pelitic-calcareous sediments, grading upwards into
291 microcrystalline limestones and lately to dolostones. Its upper section contains the
292 most extensive shallow water carbonates of the basin with laminated and columnar
293 *Gymnosolenide* stromatolites (Dardenne, 1978) and evidence for subaerial exposure
294 (Martins and Lemos 2007). Its basal contact is characterized by an unconformity: the
295 formation rests on granite-gneiss basement, on the glaciogenic Jequitáí Formation, or
296 on conglomerates of the Carrancas Formation, exposed along the southern border of
297 basin (Dardenne, 2000, Alkmin and Martins-Neto, 2001, Vieira et al. 2007).

298

299 The absence of volcanic ash horizons throughout the Bambuí, in addition to
300 hampering geochronology, has stimulated discussion regarding the tectonic setting for
301 this group (e.g. Alkmin and Martins-Neto, 2001; Zalán and Silva, 2007) and its
302 relationship with the Jequitáí diamictites (Babinski et al. 2007, 2012; Misi et al.,
303 2011; Caxito et al., 2012). A large suite of isotopic and chemostratigraphic data are
304 available (e.g. Iyer et al, 1995; Babinski et al 1999, D'Agrella-Filho et al., 2000;
305 Santos et al., 2000; Misi et al, 2007; Vieira et al. 2007), yet its depositional age
306 remains unknown. A Pb-Pb age of 740 ± 22 Ma (**Fig. 5**) from basal carbonates of the
307 Sete Lagoas Formation (Babinski et al. 2007) is the only published estimate for its
308 depositional age. In tandem with stable isotope analysis, this date led Babinski et al.
309 (2007) and Vieira et al. (2007) to propose that the Sete Lagoas is a post-Sturtian cap
310 carbonate. These interpretations contrast sharply with maximum depositional ages
311 from U-Pb detrital zircons in the upper Sete Lagoas pelites (610 Ma) (**Fig. 5**), and
312 from the overlying Serra de Santa Helena (650 Ma) and Serra da Saudade (612 Ma)
313 respectively (Rodrigues, 2008).

314

315 Detrital zircons from the underlying Jequitai Formation yield a maximum
316 depositional age of 880 Ma (Rodrigues, 2008), loosely supporting potential
317 correlation with the Sturtian glaciation, even if the depositional age of the Bambuí
318 Group, and specifically the Sete Lagoas Formation, remains highly contentious. The
319 different ages suggest a substantial hiatus. On the other hand, identical typically
320 Ediacaran $^{87}\text{Sr}/^{86}\text{Sr}$ values (0.7074-0.7076) are obtained both below and above the
321 unconformity thus arguing against a long hiatus (Caxito et al., 2012). The latter
322 authors thus interpret most of the Sete Lagoas as Ediacaran in age, with its basal strata
323 a cap carbonate deposited following the end-Cryogenian (Marinoan) glaciation.

324

325 From the above, it is clear that despite the importance in regional and global
326 studies of the Proterozoic, the understanding of the Sete Lagoas Formation sequence
327 still suffers from a lack of precise and accurate radiometric ages.

328

329 **3. Geochemistry and Re-Os geochronology methodology**

330 *3.1 Sampling*

331 Samples of the 3 formations in this study were collected from proprietary drill cores
332 (Fig. 1). The Paracatú and Serra do Garrote formations cores were provided by
333 Votorantim Mine, and a mine company from the Arcos region supplied the Sete
334 Lagoas Formation samples. In the MASW03 (Paracatú) core (Fig. 7) the sampled
335 interval spans 47.10 to 55.70 m (MD) and include dark grey to black slates, with
336 sporadic quartz as thin veins together with pyrite. VZCF001 (Serra do Garrote) core
337 samples (Fig. 8) extend from 280.10 to 292.65 m and include black slates, with
338 considerable carbonaceous material (staining). Pyrite is present, both as lamina-
339 parallel mineralization, and as crosscutting veins and framboid nodules. Finally,
340 LMR1009 (Sete Lagoas) core samples (Fig. 9) were obtained from four intervals; 1,
341 from 36-47 m (microbial dolomite and mudstones); 2, from 111-118 m (laminated
342 limestones with carbonaceous seams); 3, from 144-157 m (clay-rich limestones); 4,
343 from 158-165 m (argillites). Following Kendall et al. (2009a), ~100g samples were
344 collected at 1 m intervals in each core. Sub-sampling at further 0.4 m intervals was
345 undertaken to detect further changes in Re and Os abundance and isotope
346 composition. Care was taken to avoid zones of hydrothermal alteration and
347 mineralization.

348

349 3.2 Total organic carbon (TOC)

350 TOC values for the all samples were determined at the School of Civil Engineering
351 and Geoscience of Newcastle University, UK. An accurately weighed 0.1 g of
352 powdered rock was digested in hot (60-70°C) hydrochloric acid (4 mol/L) to remove
353 the inorganic (carbonate) carbon. The decarbonated and washed samples (in deionised
354 water) were then dried overnight in an oven at 65°C. The organic carbon in the
355 decarbonated samples was determined using a Leco CS230 Carbon-Sulphur analyser
356 (previously calibrated on standard samples), which combusted the sample in pure
357 oxygen. Any carbon present was fully oxidized and converted to CO₂ and the gaseous
358 phase was passed into an infrared detector, which measures the mass of CO₂ present
359 and converts it to percent carbon based on the dry sample weight.

360

361 3.3 Re-Os geochronology

362 For Re-Os analysis, the core samples were polished to eliminate any metal
363 contamination (e.g. cutting and drilling marks). Each sample was dried at 60 °C for
364 24h and then crushed to a powder (c. 30 µm) in a zirconium dish using an automated
365 shatterbox. Rhenium and Os isotope analyses were carried out at Durham University's
366 TOTAL laboratory for source rock geochronology and geochemistry at the Northern
367 Centre for Isotopic and Elemental Tracing (NCIET) using methods outlined in Selby
368 and Creaser (2003) and Selby (2007). Between 0.2 and 0.4 g of each sample was
369 digested and equilibrated in a borosilicate carius tube in 8 ml of Cr^{VI}-H₂SO₄ together
370 with a mixed tracer (spike) solution of ¹⁹⁰Os and ¹⁸⁵Re at 220 °C for 48 h. The Cr^{VI}-
371 H₂SO₄ solution was used to liberate hydrogenous Re and Os, restricting the
372 incorporation of non-hydrogenous Re and Os (Kendall et al., 2004). Solvent
373 extraction (CHCl₃) for Re and Os purification, micro-distillation and anion
374 chromatography methods were employed as outlined by Cumming et al., (2013). The
375 purified Re and Os fractions were loaded onto Ni and Pt filaments, respectively
376 (Selby, 2007), with the isotopic measurements determined by Negative Thermal
377 Ionization Mass Spectrometry using a Thermo Electron TRITON mass spectrometer
378 via static Faraday collection for Re and ion-counting using a secondary electron
379 multiplier in peak-hopping mode for Os. Total procedural blanks during this study
380 were 14.6 ± 0.16 pg and 0.05 ± 0.01 pg (1σ S.D., n = 3) for Re and Os, respectively,
381 with an average ¹⁸⁷Os/¹⁸⁸Os value of 0.61 ± 0.03 (n = 3). Uncertainties for ¹⁸⁷Re/¹⁸⁸Os

382 and $^{187}\text{Os}/^{188}\text{Os}$ were determined by error propagation of uncertainties in Re and Os
383 mass spectrometer measurements, blank abundances and isotopic compositions, spike
384 calibrations and reproducibility of standard Re and Os isotopic values. The Re–Os
385 isotopic data including the 2σ calculated uncertainties for $^{187}\text{Re}/^{188}\text{Os}$ and $^{187}\text{Os}/^{188}\text{Os}$
386 and the associated error correlation function (ρ) were regressed to yield a Re–Os
387 date using Isoplot V. 4.0 and the λ ^{187}Re constant of $1.666 \times 10^{-11}\text{a}^{-1}$ (Smoliar et al.,
388 1996; Ludwig, 2003). The age uncertainty including the uncertainty of 0.35 % in the
389 ^{187}Re decay constant only affects the third decimal place (Smoliar et al., 1996; Selby,
390 2007).

391

392 To evaluate mass spectrometry reproducibility, two in-house Re and Os
393 (Durham Romil Osmium Standard = DROsS) solution standards were analyzed. The
394 Re solution standard yields an average $^{185}\text{Re}/^{187}\text{Re}$ ratio of 0.598071 ± 0.001510 (1
395 S.D., $n = 67$), which is in agreement with the value reported for the AB-1 standard
396 (Rooney et al., 2010). The measured difference in $^{185}\text{Re}/^{187}\text{Re}$ values for the Re
397 standard solution and the accepted $^{185}\text{Re}/^{187}\text{Re}$ value (0.5974; Gramlich et al., 1973) is
398 used to correct the measured sample Re isotope composition. The Os isotope
399 reference solution (DROsS) gave an $^{187}\text{Os}/^{188}\text{Os}$ ratio of 0.160892 ± 0.000559 (1 S.D.,
400 $n = 67$), which is in agreement with previous studies (Rooney et al., 2010).

401

402 **4. Results**

403 *4.1 TOC*

404 The TOC results for all samples are presented in **Table 1** and **Fig. 7, 8** and **9**. The
405 Sete Lagoas Formation has the lowest TOC of the 3 analyzed cores (<0.01 to 0.49
406 wt%), while the Serra do Garrote and Paracatú formations possess the highest TOC
407 values (0.75 to 2.12% and 0.07 to 2.15 wt% respectively). According to these
408 samples, the basin possesses fair quality as a potential hydrocarbon source rock, both
409 in carbonates and shales (c.f. Craig et al., 2012). As Re-Os geochronology has been
410 applied successfully to rocks with 0.5% TOC (Kendall et al. (2004), this cut off was
411 used to select the samples for Re-Os analysis. Whole rock Rock-Eval pyrolysis
412 (Espitalié et al., 1977) permits rapid evaluation of the organic matter type, quantity
413 and maturity, however a minimum amount of organic matter is needed to obtain
414 reliable results. As only the samples from the Paracatú and Serra do Garrote
415 formations provided $\geq 1\text{wt}\%$ TOC (**Fig. 7** and **8**), in low-grade metamorphic rocks,

416 maturation analyses (Rock Eval) were not performed.

417

418 "Insert Supplementary Figure 7 here"

419 "Insert Supplementary Figure 8 here"

420 "Insert Supplementary Figure 9 here"

421 "Insert Supplementary Table 1 here"

422

423 *4.2 Paracatú Slate Formation: Re-Os data*

424 The Paracatú Slate samples have Re (0.3 – 4.1 ppb) and Os (53 – 297 ppt) abundances
425 (**Table 2**) that are close to or less than that of average continental crustal values of 1
426 ppb and 50 ppt, respectively (Esser and Turekian, 1993; Peucker-Ehrenbrink and
427 Jahn, 2001; Hattori et al., 2003). The $^{187}\text{Re}/^{188}\text{Os}$ ratios display a limited range from
428 24.2 to 79.6 and present-day $^{187}\text{Os}/^{188}\text{Os}$ ratios range from 0.667 to 1.593 (**Table 2**).
429 Regression of the Re–Os isotope data yield a Re–Os age of 1002 ± 45 Ma (2σ , $n=4$,
430 Model 1, Mean Square of Weighted Deviates [MSWD] = 1.2, initial $^{187}\text{Os}/^{188}\text{Os} =$
431 0.25 ± 0.04 ; **Fig. 10**).

432

433 "Insert Supplementary Table 2 here"

434 "Insert Supplementary Figure 10 here"

435

436 *4.3 Serra do Garrote Formation: Re-Os data*

437 The Serra do Garrote slates are enriched in Re (4 – 28 ppb) and Os (137 – 585 ppt;
438 **Table 2**) and present a large spread in $^{187}\text{Re}/^{188}\text{Os}$ ratios (205.1 - 601.2) and
439 $^{187}\text{Os}/^{188}\text{Os}$ ratios (3.628 - 12.207) (**Fig. 10**). Replicate analysis of one Serra do
440 Garrote sample (VZCF-6r) show good reproducibility in Re and Os abundances and
441 $^{187}\text{Re}/^{188}\text{Os}$ and $^{187}\text{Os}/^{188}\text{Os}$ ratios. Contrary to the Paracatú Formation, the regression
442 of the isotope data for the Serra do Garrote Formation yields an imprecise, Model 3
443 age of 1304 ± 210 Ma with a negative initial Os isotope composition of -1.0 ± 1.4 and
444 an MSWD = 96.

445

446 *4.4 Sete Lagoas Formation: Re-Os data*

447 The samples of the Sete Lagoas Formation are strongly depleted in Re, with
448 abundances <100 ppt, which are lower than estimated average (present-day) upper
449 continental crust and were not investigated further.

450

451 **5. Discussion**

452 *5.1 Paracatú Formation*

453 New Re–Os geochronology for the Paracatú Formation yields a depositional age of
454 1002 ± 45 Ma, which is in agreement, within uncertainty, of U–Pb geochronology
455 (detrital zircons ca. 1040 Ma; Valeriano et al. 2004; Rodrigues et al., 2010). This
456 relatively precise age represents the first successful application of the Re–Os system
457 in samples of this Group and the first direct depositional age geochronometer. The
458 new Re–Os geochronology data adds credence to previous studies that suggest that
459 there is no significant disturbance in the Re–Os systematics of carbonaceous organic-
460 rich rocks which have experienced low degree of metamorphism (Kendall et al., 2004;
461 Rooney et al., 2011).

462

463 Based on our Re–Os data, the Canastra Group was deposited at or around the
464 Meso-Neoproterozoic boundary. This endorses tectonostratigraphic models of a
465 passive margin sequence, deposited along the SW margin of the São Francisco-Congo
466 paleocontinent (Pimentel et al., 2001, 2011; Rodrigues et al., 2010). The dates place
467 the Canastra Group as considerably younger than the early Mesoproterozoic Paranoá
468 Group (Matteini et al., 2012), with which it has been previously correlated.

469

470 The Osi value for seawater at the time of deposition of the Paracatú Formation
471 (0.25) is much less radiogenic than the present day value (~ 1.06 ; Levasseur et al.,
472 1998) indicating that the dominant input of Os to seawater was unradiogenic. This Osi
473 value is consistent with marine Os budget dominated by extraterrestrial and
474 ultramafic-mafic magmatic / hydrothermal inputs with minor contribution of
475 dissolved radiogenic crustal Os, as has been demonstrated for Mesoproterozoic
476 seawater Os isotope composition (Kendall et al., 2009a; Rooney et al., 2010).
477 Additionally, there is a close similarity in Osi values from the Paracatú Formation
478 with the Lapa deposits (0.33 ± 0.30 ; Azmy et al. 2008). The Paracatú Formation Osi
479 provides an important additional datapoint to that available for Precambrian seawater,
480 indicating that the change in global patterns of oxidative weathering and Os influx
481 was of little importance, at least until the Tonian.

482

483 Considering the amount of organic matter preserved even after maturation, it

484 is likely that the Paracatú Formation of the Canastra Group constituted an extensive
485 hydrocarbon source rock. Despite no remaining potential for further hydrocarbon
486 generation, it is not implausible that between deposition (~1000 Ma) and prior to the
487 last tectono-metamorphic event recognised in the Brasília Belt (ca. 600 Ma; Pimentel
488 et al., 1999), the rock expelled hydrocarbons. However, the data available is
489 insufficient to determine the precise timing of generation / migration, as the intense
490 deformation during the Brasiliano-Pan African events and the posthumous erosion has
491 obliterated true stratigraphic thicknesses and has conditioned seismic imaging.

492

493 *5.2 Serra do Garrote Formation*

494 Although the Paracatú Formation experienced regional metamorphism, these samples
495 yield a nominally precise depositional age with a low degree of scatter about the
496 linear regression of the Re–Os data (1002 ± 45 Ma, MSWD = 1.2). In contrast, the
497 Serra do Garrote Formation which has also experienced regional Brasiliano
498 metamorphic event (Dardenne, 2000) show a large scatter about the Re–Os regression
499 line (Model 3, 1304 ± 210 , MSWD = 96) together with a negative initial Os isotope
500 composition (-1.0 ± 1.4) suggestive of disturbances to the Re–Os systematics. This
501 imprecise age may result from either depositional and/or post-depositional processes.
502 The presence of detrital Os with variable initial $^{187}\text{Os}/^{188}\text{Os}$ composition, which tends
503 to induce imprecise and geologically meaningless ages (Kendall et al., 2004, 2009a),
504 is considered unlikely because the $\text{Cr}^{\text{VI}}\text{-H}_2\text{SO}_4$ digestion technique used in this study
505 has successfully allowed the generation of Model 1 ages for organic-rich rocks
506 containing low Re and Os abundances (Kendall et al., 2004, 2006, 2009a; Rooney et
507 al., 2011). Another feasible cause of geological uncertainty for the Re–Os systematics
508 can be represented by variations in seawater Os isotope compositions during
509 deposition (Selby and Creaser, 2003). In order to avoid heterogeneity in the
510 contemporaneous seawater Os isotope composition, short stratigraphic sampling
511 intervals (~0.6 m) were used. Os isotope composition, however, show variations that
512 span far beyond those expected from temporal evolution in seawater (unless
513 sedimentation rates were anomalously low). Thus, these variations may not fully
514 account for the complex Re–Os systematics in the Serra do Garrote Formation.

515

516 Weathering and metamorphism are unlikely explanations for the scattered Re-

517 Os isotope systematics because drill core samples were used for the analysis.
518 Additionally, metamorphic conditions of the Serra do Garrote Formation related to the
519 Brasiliano-Pan African Orogeny did not exceed greenschist facies (Dardenne, 2000;
520 Misi et al., 2005, 2007). Petrologic evidence (coarse pyrite aggregates, quartz veinlets
521 and pervasive faulting and fracturing) suggests the Serra do Garrote Formation has
522 been affected by hydrothermal fluid flow. Although we avoided sampling material
523 with abundant quartz veins, the scatter in the Re–Os regressions for the Serra do
524 Garrote Formation and the Osi signature of the samples is indicative of a
525 hydrothermal alteration origin, implying that there might have been some
526 mobilization of Re and Os by fluid flow. Similar Re-Os behavior has been observed
527 by Rooney et al., (2011) for the Leny Limestone and by Kendall et al., (2009b) for the
528 Wologorang Formation. Although the Vazante Ore deposit is located in the overlying
529 Serra do Poço Verde Formation (Soares Monteiro et al., 2006), we do not discount the
530 possibility that the same mineralizing and oxidant fluids may have affected the unit
531 under study due to the proximity of well VZCF001 to brecciated metadolomites and
532 epigenetic willemitic ore bodies along the Vazante Shear Zone (**Fig. 1B**). Therefore, it
533 is possible that the high-temperature (> 250°C), oxidizing and moderate saline (~ 15
534 wt. % NaCl equiv.) brines that leached base metals from the basement and ascended
535 to finally interact with the host dolostones of the Serra do Poço Verde (Monteiro et
536 al., 2003; Misi et al., 2005) have hydrated the Serra do Garrote slates, resulting in
537 disturbance of the Re–Os geochronometer.

538

539 It is likely that the extensive hydrothermal activity recorded in the Vazante
540 Group, and associated with the abundant Zn deposits (Soares Monteiro et al., 2006)
541 had intrinsic relation with hydrocarbon generation, possibly sourced by the Serra do
542 Garrote Formation. Pyrobitumen has been observed within hydrothermal veins in the
543 carbonates of the overlying Morro do Calcário Formation (Rubo and Soares Monteiro,
544 2010; Tonietto, 2011) and hydrocarbon inclusions were described in sulfides of the
545 Vazante ore deposit (L. Soares Monteiro pers. comm.). Future dating of these
546 hydrocarbon products with the ^{187}Re - ^{187}Os radioisotope system (e.g., Selby and
547 Creaser, 2005b) could help constraining the timing of emplacement, the source of
548 migrated hydrocarbons and the temporal relation of the mineralization and
549 hydrocarbon accumulation.

550

551

552 *5.3 Sete Lagoas Formation*

553 The lack of Re in the carbonate of the Sete Lagoas could be intrinsically associated
554 with the low TOC observed for the unit. Re and Os are organophilic and redox-
555 sensitive, therefore in reducing pore waters Re is removed at the sediment–water
556 interface, remaining physically associated with organic matter (Selby & Creaser 2003,
557 Kendall et al., 2004, 2009a and refs therein). If the sediments lacked enough organic
558 matter and / or if the environment of deposition was neither euxinic nor anoxic, it is
559 likely that hydrogenous Os was not incorporated into the sediments. On the other
560 hand, the observed low organic content can also be related to thermal maturation
561 (Peters and Cassa, 1994) which may cause as a loss of 30-50% of the assumed
562 original amount of TOC (Buchardt et al., 1986). With the intention of accounting for
563 the effects of maturation, biomarkers studies were performed by the author. However,
564 results proved inconclusive likely due to low volumes of organic matter analysed.

565

566 Several isotopic studies have demonstrated negative excursion of $\delta^{13}\text{C}$ and ^{18}O
567 for the base of the Sete Lagoas Formation (Alvarenga et al., 2007; Kuchenbecker,
568 2011). This behaviour, together with its stratigraphic position, sitting on top of the
569 Jequitaí diamictite deposits, led to interpretations of a typical postglacial cap
570 carbonate sequence related either to Sturtian (Babinski et al. 2007; Babinski and
571 Kaufman, 2003) or Marinoan (Caxito et al., 2012) deglaciation.

572

573 The recognition of palaeovalleys on seismic and outcrop data (Martins-
574 Ferreira et al. 2013) and information of their infill with the Jequitaí Diamictites and
575 Bambuí dolomites has important implications. Bechstädt et al. (2009) provided TOC
576 data from the Maieberg Formation in northern Namibia, a laminated cap dolostone
577 sitting on top of the Ghaub Formation diamictite, and which corresponds to a late
578 Cryogenian (“Marinoan”) glacial deposit. Noting that there is local enrichment of
579 TOC in the dololaminites, Bechstädt et al. (2009) draw on analogues of deglaciation
580 from the Lower Palaeozoic of North Africa to explain this phenomenon. Deglaciation
581 from the Hirnantian ice age left behind a complex, glacially sculpted topography
582 produced by a combination of subglacial abrasion and meltwater. Accumulation of
583 organic material, with primary productivity stimulated by meltwater release and
584 aeolian dust (Gabbott et al. 2010), occurred. During transgression, however,

585 palaeovalleys were flooded first. Initially, these were disconnected from one another,
586 and thus euxinic to anoxic conditions developed. Later during the transgression,
587 organic-lean shales were deposited as circulation resumed and palaeovalleys were
588 overspilled (Lüning et al., 2000). The presence of lingering ice sheets lowered the
589 preservation potential of organic material, because oxygen-rich brines released during
590 sea ice production diminish euxinia at the sea floor (Le Heron et al., 2013). Thus, by
591 analogy, the distribution of TOC enrichment in Cryogenian post-glacial deposits has
592 been hard to predict (Bechstädt et al. 2009). If the base of the Sete Lagoas Formation
593 was deposited under these circumstances, some of the complex factors linked to
594 restricted / open circulation within / out palaeovalleys may explain oxidizing versus
595 anoxic conditions for organic preservation and associated Rhenium complexation.
596 The lack of diamictites underlying the carbonates of the Sete Lagoas Formation in
597 well LMR1009 (opposed to other cores of the region; F. Pimenta pers. comm.) could
598 indicate its position away from a paleodepression (**Fig. 11**), justifying the low TOC
599 values observed in this particular location. This interpretation can only be tentative,
600 however, because the location of the well used for this analysis is not imaged in
601 seismic section. Nevertheless, considering that post-glacial shales in North Africa,
602 have charged more than 50 major oil and gas fields (Lüning et al., 2000), and that
603 enrichment of up to ~6% TOC has been reported in other parts of the basin for the Sete
604 Lagoas Formation (Iyer et al., 1995), it is likely that post-Jequitaí sediments might
605 represent a hydrocarbon source rock interval.

606

607 "Insert Supplementary Figure 11 here"

608

609 **6. Conclusions**

610

- 611 • New Re–Os geochronology for the Paracatú Formation yields a depositional
612 age of 1002 ± 45 Ma and is in agreement, within uncertainty, of U–Pb detrital
613 geochronology. This relatively precise age coupled with the excellent linear fit
614 of the Re–Os isotope data provides a more precise chronostratigraphic
615 framework for understanding the tectonic evolution of the Canastra Group and
616 the onset of sedimentation within the basin.

617

- 618 • Disturbance of Re–Os systematics in the Serra do Garrote Formation is
619 evident by a very imprecise and inaccurate age along with a negative value for
620 the Osi value. These factors together with petrological evidence strongly
621 suggest that the Re–Os system was disturbed in response to hydrothermal fluid
622 flow, possibly associated with the mineralized bodies of the Vazante ore
623 deposits. The circulation of fluids through the Vazante Group is suggested to
624 be the cause for the gain of Re and Os and loss of reliable depositional age
625 information. Care is consequently necessary when applying the Re–Os
626 deposition-age geochronometer to sedimentary rocks subject to tectonic
627 deformation and affected by hydrothermal fluids.
628
- 629 • The lack of Rhenium enrichment in the base of the Sete Lagoas Formation
630 could be explained by the control on the distribution of the organically enrich
631 facies which, similarly to the Early Silurian deglacial shales (Luñing et al.,
632 2000), was inherited from glacial topography, and is directly related to
633 incisions cut during ice advance and ice retreat.

634
635

636 **Acknowledgements**

637

638 This research was generously funded by a grant from Sonangol to Daniel P. Le Heron,
639 supporting the doctoral research of the first author and the AAPG Foundation Gordon
640 I. Atwater Grant awarded to MEB. The Brazilian Council for Scientific and
641 Technological Development- CNPq provided a reaserch grant to F.F.Alkmim (Grant
642 #307531/2009-0). Votorantim mine and a mining company from Arcos region, are
643 thanked for provision of core samples and particular Samuel Boucas do Lago,
644 Gustavo Diniz Oliveira, Leonardo Lopes-Silva and Felipe Pimenta are thanked for
645 their assistance with the sample collection.

646

647

648

649 **References**

650

651 Alkmim, F. F., & Martins-Neto, M. A., 2001. A Bacia intracratônica do São
652 Francisco: Arcabouço estrutural e cenários evolutivos. Bacia do São Francisco:
653 geologia e recursos naturais. SBG-MG, Belo Horizonte, 9-30.

654

655 Alkmim, F. F., Marshak, S., & Fonseca, M. A., 2001. Assembling West Gondwana in
656 the Neoproterozoic: clues from the São Francisco craton region, Brazil. *Geology*,
657 29(4), 319-322.

658

659 Alkmim, F. F., & Martins-Neto, M. A., 2012. Proterozoic first-order sedimentary

660 sequences of the São Francisco craton, eastern Brazil. *Marine and Petroleum*
661 *Geology*, 33(1), 127-139.

662

663 Almeida, F. F. M. D., Brito Neves, B. B. D., & Dal Ré Carneiro, C., 2000. The origin
664 and evolution of the South American Platform. *Earth-Science Reviews*, 50(1), 77-111.

665

666 Alvarenga, C.J.S., Della Giustina, M.E.S., Silva, M.G.C., Santos, R.V., Gioia,
667 S.M.C., Guimarães, E.M., Dardenne, M.A., Sial, A.N., Ferreira, V.P., 2007. Variaç
668 ões dos isótopos de C e Sr em carbonatos pré e pós-glaciac, ão Jequitaiá (Esturtiano)
669 na região de Bezerra-Formosa, Goiás. *Revista Brasileira de Geociências* 37, 147–155.

670

671 Azmy, K., Kaufman, A. J., Misi, A., & Oliveira, T. F. D., 2006. Isotope stratigraphy
672 of the Lapa formation, São Francisco basin, Brazil: implications for late
673 Neoproterozoic glacial events in South America. *Precambrian Research*, 149(3), 231-
674 248.

675

676 Azmy, K., Kendall, B., Creaser, R. A., Heaman, L., & de Oliveira, T. F., 2008. Global
677 correlation of the Vazante Group, São Francisco Basin, Brazil: Re–Os and U–Pb
678 radiometric age constraints. *Precambrian Research*, 164(3), 160-172.

679

680 Babinski, M., Van Schmus, W. R., & Chemale Jr, F., 1999. Pb–Pb dating and Pb
681 isotope geochemistry of Neoproterozoic carbonate rocks from the São Francisco
682 basin, Brazil: implications for the mobility of Pb isotopes during tectonism and
683 metamorphism. *Chemical Geology*, 160(3), 175-199.

684

685 Babinski, M., Kaufman, A. J., and Varni, M., 2003. First direct dating of a
686 Neoproterozoic post-glacial cap carbonate. *South American Symposium on Isotope*
687 *Geology*. Vol. 4.

688

689 Babinski, M., Monteiro, L. V. S., Fetter, A. H., Bettencourt, J. S., & Oliveira, T. F.,
690 2005. Isotope geochemistry of the mafic dikes from the Vazante nonsulfide zinc
691 deposit, Brazil. *Journal of South American Earth Sciences*, 18(3), 293-304.

692

693 Babinski, M., Vieira, L. C., & Trindade, R. I., 2007. Direct dating of the Sete Lagoas
694 cap carbonate (Bambuá Group, Brazil) and implications for the Neoproterozoic glacial
695 events. *Terra Nova*, 19(6), 401-406.

696

697 Babinski, M., Pedrosa-Soares, A. C., Trindade, R. I. F., Martins, M., Noce, C. M., &
698 Liu, D., 2012. Neoproterozoic glacial deposits from the Araçuaí orogen, Brazil: Age,
699 provenance and correlations with the São Francisco craton and West Congo belt.
700 *Gondwana Research*, 21(2), 451-465.

701

702 Bechstädt, T., Jäger, H., Spence, G. & Werner, G., 2009. Late Cryogenian
703 (Neoproterozoic) glacial and post-glacial successions at the southern margin of the
704 Congo Craton, northern Namibia: facies, palaeogeography and hydrocarbon
705 perspective. In: Craig, J., Thurow, J., Thusu, B., Whitham, A. & Abutarruma, Y. (eds)
706 *Global Neoproterozoic Petroleum Systems: The Emerging Potential in North Africa*.
707 Geological Society, London, Special Publications, 326, 255–287.

708

709 Buchardt, B., Clausen, J., & Thomsen, E., 1986. Carbon isotope composition of

710 Lower Palaeozoic kerogen: effects of maturation. *Organic geochemistry*, 10(1), 127-
711 134.
712
713 Caxito, F. D. A., Halverson, G. P., Uhlein, A., Stevenson, R., Gonçalves Dias, T., &
714 Uhlein, G. J., 2012. Marinoan glaciation in east central Brazil. *Precambrian Research*,
715 200, 38-58.
716
717 Chaves, M. L. D. S. C., Guimarães, J. T., & Andrade, K. W. 2010. Glaciomarine
718 lithofacies in the Jequitá Formation: possible implications for the redistribution of
719 diamonds to the west of the Espinhaço Range (MG). *Revista Brasileira de*
720 *Geociências*, 40(4), 516-526.
721
722 Cohen, A. S., Coe, A. L., Bartlett, J. M., & Hawkesworth, C. J. 1999. Precise Re–Os
723 ages of organic-rich mudrocks and the Os isotope composition of Jurassic seawater.
724 *Earth and Planetary Science Letters*, 167(3), 159-173.
725
726 Craig, J., Biffi, U., Galimberti, R. F., Ghorri, K. A. R., Gortler, J., Hakhoo, N., Le
727 Heron D. P., Thurow J. & Vecoli, M., 2012. The palaeobiology and geochemistry of
728 Precambrian hydrocarbon source rocks. *Marine and Petroleum Geology*.
729
730 Cukrov, N., De Alvarenga, C.J.S. & Uhlein, A., 2005. Litofácies da glaciação
731 Neoproterozóica nas porções sul do cráton do São Francisco: Exemplos de Jequitá
732 (MG) e Cristalina (Go). *Revista Brasileira de Geociências*, 35, 69-76.
733
734 Cumming, V. M., Selby, D., & Lillis, P. G., 2012. Re–Os geochronology of the
735 lacustrine Green River Formation: Insights into direct depositional dating of lacustrine
736 successions, Re–Os systematics and paleocontinental weathering. *Earth and Planetary*
737 *Science Letters*, 359, 194-205.
738
739 Cumming, V.M, Poulton, S.W., Rooney, A.D. & Selby, D., 2013. Anoxia in the
740 terrestrial environment during the Late Mesoproterozoic. *Geology* 41(5): 583-586.
741
742 D'Agrella-Filho, M. S., Babinski, M., Trindade, R. I. F., Van Schmus, W. R., &
743 Ernesto, M., 2000. Simultaneous remagnetization and U–Pb isotope resetting in
744 Neoproterozoic carbonates of the Sao Francisco craton, Brazil. *Precambrian Research*,
745 99(3), 179-196.
746
747 Dardenne, M. A., 1978. Síntese sobre a estratigrafia do Grupo Bambuí no Brasil
748 Central. *SBG, Congr. Bras. Geol*, 30, 507-610.
749
750 Dardenne, M.A., 2000. The Brasília fold belt. In: Cordani, U.G., Milani, E.J., Thomaz
751 Filho, A., Campos, D.A. (Eds.), *Tectonic Evolution of South America*. 31st
752 *International Geological Congress*, Rio de Janeiro, pp. 231-263.
753
754 Espitalié J., La Porte J.L., Madec M., Marquis F., Le Plat P., Paulet J. & Boutefeu A.,
755 1977. Rapid method for source rocks characterization and for determination of
756 petroleum potential and degree of evolution. *Oil and Gas Science and Technology-*
757 *Revue de l'Institut Français du Pétrole*, 32, 23-42.
758
759 Esser, B. K., & Turekian, K. K., 1993. The osmium isotopic composition of the

760 continental crust. *Geochimica et Cosmochimica Acta*, 57(13), 3093-3104.
761
762 Freitas-Silva, F. H., 1996. Metalogênese do depósito do Morro do Ouro, Paracatú,
763 MG. Tese de Doutorado, IG/UnB, Brasília, 339.
764
765 Gabbott, S.E., Zalasiewicz, J.A., Aldridge, R.J., & Theron, N., 2010. Eolian input into
766 the Late Ordovician postglacial Soom Shale, South Africa. *Geology*, 38(12), 1103-
767 1106.
768
769 Geboy, N. J., 2006. Rhenium-Osmium Age Determinations of Glaciogenic Shales
770 from the Mesoproterozoic Vazante Formation, Brazil (Master dissertation).
771
772 Georgiev, S., Stein, H. J., Hannah, J. L., Bingen, B., Weiss, H. M., & Piasecki, S.,
773 2011. Hot acidic Late Permian seas stifled life in record time. *Earth and Planetary
774 Science Letters*, 310(3), 389-400.
775
776 Gramlich, J.W., Murphy, T.J., Garner, E.L., Shields, W.R., 1973. Absolute isotopic
777 abundance ratio and atomic weight of a reference sample of rhenium. *Nat. Bur. Stds.
778 J. Res.*, 77A, 691–698.
779
780 Hattori, Y., Suzuki, K., Honda, M., & Shimizu, H., 2003. Re-Os isotope systematics
781 of the Taklimakan Desert sands, moraines and river sediments around the Taklimakan
782 Desert, and of Tibetan soils. *Geochimica et cosmochimica acta*, 67(6), 1203-1213.
783
784 Iyer, S. S., Babinski, M., Krouse, H. R., & Chemale Jr, F., 1995. Highly ¹³C-enriched
785 carbonate and organic matter in the Neoproterozoic sediments of the Bambuí Group,
786 Brazil. *Precambrian Research*, 73(1), 271-282.
787
788 Kendall B. S., Creaser R. A., Ross G. M. and Selby D., 2004. Constraints on the
789 timing of Marinoan “Snowball Earth” glaciation by ¹⁸⁷Re–¹⁸⁷Os dating of a
790 Neoproterozoic, post- glacial black shale in Western Canada. *Earth Planet. Sci. Lett.*
791 222, 729–740
792
793 Kendall, B., Creaser, R.A., 2006. Re–Os systematics of the Proterozoic Velkerri and
794 Wollongorang black shales, McArthur Basin, northern Australia. In: *Goldschmidt
795 Conference (Abstract)*, Melbourne, Australia.
796
797 Kendall, B., Creaser, R. A., & Selby, D., 2009a. ¹⁸⁷Re–¹⁸⁷Os geochronology of
798 Precambrian organic-rich sedimentary rocks. *Geological Society, London, Special
799 Publications*, 326(1), 85-107.
800
801 Kendall, B., Creaser, R. A., Gordon, G. W., & Anbar, A. D. 2009b. Re–Os and Mo
802 isotope systematics of black shales from the Middle Proterozoic Velkerri and
803 Wollongorang formations, McArthur Basin, northern Australia. *Geochimica et
804 Cosmochimica Acta*, 73(9), 2534-2558.
805
806 Kuchenbecker, M., 2011. Químioestratigrafia e proveniência sedimentar da porção
807 basal do Grupo Bambuí em Arcos (MG). Masters Dissertation, IGC–Universidade
808 Federal de Minas Gerais, Belo Horizonte, Brazil, 91 p.
809

810 Levasseur, S., Birck, J. L. & Allègre, C. J., 1998. Direct measurement of femtomoles
811 of osmium and the $^{187}\text{Os}/^{186}\text{Os}$ ratio in seawater. *Science*, 282(5387), 272-274.
812

813 Li, Z. X., Bogdanova, S. V., Collins, A. S., Davidson, A., De Waele, B., Ernst, R. E.,
814 Fitzsimons, I. C. W., Fuck R. A., Gladkochub, D. P., Jacobs, J., Karlstrom, K. E., Lu
815 S., Natapov, L. M., Pease, S. A., Pisarevsky, S. A., Thrane, K., & Vernikovsky, V.,
816 2008. Assembly, configuration, and break-up history of Rodinia: a synthesis.
817 *Precambrian Research*, 160(1), 179-210.
818

819 Le Heron, D. P., Busfield, M. E., & Kamona, F., 2012. An interglacial on snowball
820 Earth? Dynamic ice behaviour revealed in the Chuos Formation, Namibia.
821 *Sedimentology*.
822

823 Le Heron, D.P., Meinhold, G., Page, A.A., Whitham, A.G., 2013. Did lingering ice
824 sheets moderate anoxia in the Early Palaeozoic of Libya? *Journal of the Geological*
825 *Society of London*, 170, 327-339.
826

827 Lonergan, L., Maidment, S. C., & Collier, J. S., 2006. Pleistocene subglacial tunnel
828 valleys in the central North Sea basin: 3-D morphology and evolution. *Journal of*
829 *Quaternary Science*, 21(8), 891-903.
830

831 Ludwig, K., 2003. Isoplot/Ex, Version 3: A Geochronological Toolkit for Microsoft
832 Excel. Geochronology Center Berkeley.
833

834 Lüning, S., Craig, J., Loydell, D. K., Storch, P. & Fitches, W., 2000. Lowermost
835 Silurian 'hot shales' in north Africa and Arabia: regional distribution and depositional
836 model. *Earth Science Reviews*, 49, 121–200.
837

838 Macdonald, F. A., Schmitz, M. D., Crowley, J. L., Roots, C. F., Jones, D. S., Maloof,
839 A. C., Strauss, J. V., Cohen, P. A., Johnston, D. T., & Schrag, D. P., 2010. Calibrating
840 the Cryogenian. *Science*, 327 (5970), 1241-1243.
841

842 Madalosso, A. & Valle, C.R.O., 1978. Considerações sobre a estratigrafia e
843 sedimentologia do Grupo Bambuí na região de Paracatu-Morro Agudo (MG). In: 30
844 Congresso Brasileiro de Geologia, Anais, 622-631.
845

846 Madalosso, A., 1980. Considerações sobre a paleogeografia do Grupo Bambuí na
847 região de Paracatu – Morro Agudo (MG). In: 31 Congresso Brasileiro de Geologia,
848 Anais, (2), 772-785.
849

850 Mahan, K. H., Wernicke, B. P., & Jercinovic, M. J., 2010. Th–U–total Pb
851 geochronology of authigenic monazite in the Adelaide rift complex, South Australia,
852 and implications for the age of the type Sturtian and Marinoan glacial deposits. *Earth*
853 *and Planetary Science Letters*, 289(1), 76-86.
854

855 Martins, M., & Lemos, V. B., 2007. Análise estratigráfica das seqüências
856 neoproterozóicas da Bacia do São Francisco. *Brazilian Journal of Geology*, 37(4),
857 156-167.
858

859 Martins-Ferreira, M.A.; Campos, J.E.G.& Alvarenga, C. J.S. 2013. A Formação

860 Jequitai na região de Vila Boa, GO: exemplo de sedimentação por geleiras terminais
861 no Neoproterozóico. *Brazilian Journal of Geology*, 43(2):373-384.
862

863 Martins-Neto, M. A., 2009. Sequence stratigraphic framework of Proterozoic
864 successions in eastern Brazil. *Marine and Petroleum Geology*, 26(2), 163-176.
865

866 Matteini, M., Dantas, E. L., Pimentel, M. M., de Alvarenga, C. J. S., & Dardenne, M.
867 A., 2012. U–Pb and Hf isotope study on detrital zircons from the Paranoá Group,
868 Brasília Belt Brazil: Constraints on depositional age at Mesoproterozoic–
869 Neoproterozoic transition and tectono-magmatic events in the São Francisco craton.
870 *Precambrian Research*, 206, 168-181.
871

872 Misi, A., Iyer, S.S., Coelho, C.E.S., Tassinari, C.C.G., Franca-Rocha, W.J.S., Cunha,
873 I.A., Gomes, A.S.R., Oliveira, T.F., Teixeira, J.B.G., Filho, V.M., 2005. Sediment
874 hosted lead–zinc deposits of the Neoproterozoic Bambuí Group and correlative
875 sequences, São Francisco Craton, Brazil: a review and a possible metallogenic
876 evolution model. *Ore Geology Reviews* 26, 263–304.
877

878 Misi, A., Kaufman, A.J., Veizer, J., Powis, K., Azmy, K., Boggiani, P.C., Gaucher,
879 C., Teixeira, J.B.G., Sanches, A.L., Iyer, S.S.S., 2007. Chemostratigraphic correlation
880 of Neoproterozoic successions in South América. *Chemical Geology* 237 (2007) 143–
881 167
882

883 Misi, A., Kaufman, A. J., Azmy, K., Dardenne, M. A., Sial, A. N., & de Oliveira, T.
884 F., 2011. Neoproterozoic successions of the São Francisco craton, Brazil: the Bambuí,
885 Una, Vazante and Vaza Barris/Miaba groups and their glaciogenic deposits.
886 *Geological Society, London, Memoirs*, 36(1), 509-522.
887

888 Monteiro, L. V. S., Bettencourt, J. S., Bello, R. M. S., Juliani, C., Tassinari, C. C. G.,
889 Oliveira, T. F., & Pérez-Aguillar, A., 2003. Sulfur, carbon, oxygen and strontium
890 isotopic evidences for the genesis of the hydrothermal zinc non-sulfide and sulfide
891 mineralizations in the Vazante, Ambrosia and Fagundes deposits, MG, Brazil. In
892 *Short Papers IV South American Symposium on Isotope Geology* (pp. 748-751).
893

894 Olcott, A. N., Sessions, A. L., Corsetti, F. A., Kaufman, A. J., & De Oliviera, T. F.,
895 2005. Biomarker evidence for photosynthesis during Neoproterozoic glaciation.
896 *Science*, 310(5747), 471-474.
897

898 Pedrosa-Soares, A.C., Cordani, U. & Nutman, A., 2000. Constraining the age of
899 Neoproterozoic glaciation in eastern Brazil: first U-Pb (SHRIMP) data from detrital
900 zircons. *Revista Brasileira de Geociências* 30, 58-61.
901

902 Pereira, L. F., Dardenne, M. A., Rosière, C. A., & Pedrosa-Soares, A. C., 1994.
903 Evolução geológica dos grupos Canastra e Ibia na região entre Coromandel e Guarda-
904 Mor, MG. *Revista Geonomos*, 2(1).
905

906 Peters, K. E., & Cassa, M. R., 1994. Applied source rock geochemistry. *Memoirs-*
907 *American Association of Petroleum Geologists*, 93-93.
908

909 Peucker-Ehrenbrink, B., & Jahn, B. M., 2001. Rhenium-osmium isotope systematics

910 and platinum group element concentrations: Loess and the upper continental crust.
911 Geochemistry, Geophysics, Geosystems, 2(10).
912
913 Pimentel, M. M., Fuck, R. A., & Botelho, N. F., 1999. Granites and the geodynamic
914 history of the Neoproterozoic Brasília belt, central Brazil: a review. *Lithos*, 46(3),
915 463-483.
916
917 Pimentel, M., Dardenne, M., Fuck, R., Viana, M., Junges, S. L., Fischel, D. P., Seer,
918 H.J., & Dantas, E. L., 2001. Nd isotopes and the provenance of detrital sediments of
919 the Neoproterozoic Brasília Belt, central Brazil. *Journal of South American Earth
920 Sciences*, 14(6), 571-585.
921
922 Pimentel, M. M., Rodrigues, J. B., DellaGiustina, M. E. S., Junges, S., Matteini, M.,
923 & Armstrong, R., 2011. The tectonic evolution of the Neoproterozoic Brasília Belt,
924 central Brazil, based on SHRIMP and LA-ICPMS U–Pb sedimentary provenance
925 data: A review. *Journal of South American Earth Sciences*, 31(4), 345-357.
926
927 Ravizza, G., & Turekian, K. K., 1989. Application of the ^{187}Re - ^{187}Os system to black
928 shale geochronometry. *Geochimica et Cosmochimica Acta*, 53(12), 3257-3262.
929
930 Rodrigues, J. B., 2008. Proveniência de sedimentos dos grupos Canastra, Ibiá,
931 Vazante e Bambuí e Um estudo de zircões detríticos e Idades Modelo Sm-Nd.
932 Doctorate Thesis, Univ. Brasília, 141p.
933
934 Rodrigues, J. B., Pimentel, M. M., Dardenne, M. A., & Armstrong, R. A., 2010. Age,
935 provenance and tectonic setting of the Canastra and Ibiá Groups (Brasília Belt,
936 Brazil): Implications for the age of a Neoproterozoic glacial event in central Brazil.
937 *Journal of South American Earth Sciences*, 29(2), 512-521.
938
939 Rodrigues, J. B., Pimentel, M. M., Buhn, B., Matteini, M., Dardenne, M. A.,
940 Alvarenga, C. J. S., & Armstrong, R. A., 2012. Provenance of the Vazante Group:
941 New U–Pb, Sm–Nd, Lu–Hf isotopic data and implications for the tectonic evolution
942 of the Neoproterozoic Brasília Belt. *Gondwana Research*, 21(2), 439-450.
943
944 Rooney, A. D., Selby, D., Houzay, J. P., & Renne, P. R., 2010. Re–Os geochronology
945 of a Mesoproterozoic sedimentary succession, Taoudeni basin, Mauritania:
946 Implications for basin-wide correlations and Re–Os organic-rich sediments
947 systematics. *Earth and Planetary Science Letters*, 289(3), 486-496.
948
949 Rooney, A. D., Chew, D. M., & Selby, D., 2011. Re–Os geochronology of the
950 Neoproterozoic–Cambrian Dalradian supergroup of Scotland and Ireland:
951 implications for Neoproterozoic stratigraphy, glaciations and Re–Os systematics.
952 *Precambrian Research*, 185(3), 202-214.
953
954 Rooney, A.D., Macdonald, F.A., Strauss, J.V., Dudás, F. Ö., Hallmann, C., Selby, D.
955 in press. Weathering the Snowball. *Proceedings of the National Academy of Sciences*.
956
957 Santos, R. V., De Alvarenga, C. J. S., Dardenne, M. A., Sial, A. N., & Ferreira, V. P.,
958 2000. Carbon and oxygen isotope profiles across Meso-Neoproterozoic limestones
959 from central Brazil: Bambuí and Paranoá groups. *Precambrian Research*, 104(3), 107-

960 122.
961
962 Selby, D., & Creaser, R. A., 2003. Re–Os geochronology of organic rich sediments:
963 an evaluation of organic matter analysis methods. *Chemical Geology*, 200(3), 225-
964 240.
965
966 Selby, D., & Creaser, R. A., 2005a. Direct radiometric dating of the Devonian-
967 Mississippian time-scale boundary using the Re-Os black shale geochronometer.
968 *Geology*, 33(7), 545-548.
969
970 Selby, D., & Creaser, R. A., 2005b. Direct radiometric dating of hydrocarbon deposits
971 using rhenium-osmium isotopes. *Science*, 308(5726), 1293-1295.
972
973 Selby, D., Creaser, R. A., Dewing, K., & Fowler, M., 2005. Evaluation of bitumen as
974 a ^{187}Re – ^{187}Os geochronometer for hydrocarbon maturation and migration: A test
975 case from the Polaris MVT deposit, Canada. *Earth and Planetary Science Letters*, 235
976 (1), 1-15.
977
978 Selby, D., 2007. Direct Rhenium-Osmium age of the Oxfordian-Kimmeridgian
979 boundary, Staffin bay, Isle of Skye, UK, and the Late Jurassic time scale. *Norsk*
980 *Geologisk Tidsskrift*, 87(3), 291.
981
982 Smoliar, M.I., Walker, R.J., Morgan, J.W., 1996. Re-Os isotope constraints on the age
983 of Group IIA, IIIA, IVA, and IVB iron meteorites. *Science* 271, 1099-1102.
984
985 Soares Monteiro, L. V., Bettencourt, J. S., Juliani, C., & de Oliveira, T. F., 2006.
986 *Geology, petrography, and mineral chemistry of the Vazante non-sulfide and*
987 *Ambrósia and Fagundes sulfide-rich carbonate-hosted Zn–(Pb) deposits, Minas*
988 *Gerais, Brazil. Ore Geology Reviews*, 28(2), 201-234.
989
990 Stewart, M. A., & Lonergan, L., 2011. Seven glacial cycles in the middle-late
991 Pleistocene of northwest Europe: Geomorphic evidence from buried tunnel valleys.
992 *Geology*, 39(3), 283-286.
993
994 Rubo, R. A., & Monteiro, L. V. S., 2010. Sistemática de isótopos de oxigênio e
995 carbono aplicada ao estudo da evolução metalogenética do depósito de Zn-Pb de
996 Morro Agudo (MG). *Brazilian Journal of Geology*, 40(3), 438-452.
997
998 Tonietto, S. N., 2011. *Diagênese e hidrotermalismo em rochas carbonáticas*
999 *proterozóicas: Grupos Bambuí e Vazante, Bacia do São Francisco. MSc Thesis. Univ.*
1000 *Brasília, 196p.*
1001
1002 Valeriano, C.M., Machado, N., Simonetti, A., Valladares, C.S., Seer, H.J., Simões,
1003 L.S.A., 2004. U-Pb geochronology of the Southern Brasília belt (SE-BRAZIL):
1004 sedimentary provenance, Neoproterozoic Orogeny and assembly of West Gondwana.
1005 *Precambrian Research* 130, 27-55.
1006
1007 Valeriano, C.M., Pimentel, M.M., Heilbron, M., Almeida, J.C.H., Trouw, R.A.J.,
1008 2008. Tectonic evolution of the Brasília belt, central Brazil, and early assembly of
1009 Gondwana. In: Pankhurst, R.J., Trouw, R.A.J., Brito Neves, B.B., De Wit, M.J.

- 1010 (Eds.), West Gondwana: Pre-cenozoic Correlations across the South Atlantic Region.
1011 Geological Society, London, Special Publications, vol. 294, pp. 197-210.
1012
- 1013 Uhlein, A., Trompette, R.R., Egydio-Silva, M., Vauhez, M., 2007. A glaciação
1014 Sturtiana (~750 Ma), a estrutura do rifte Macaúbas Santo Onofre e a estratigrafia do
1015 Grupo Macaúbas, Faixa Araçuaí. Geonomos, 15, 45-60.
1016
- 1017 Van der Vegt, P., Janszen, A., & Moscariello, A., 2012. Tunnel valleys: current
1018 knowledge and future perspectives. Geological Society, London, Special Publications,
1019 368(1), 75-97.
1020
- 1021 Vieira, L. C., Almeida, R. P., Trindade, R. I., Nogueira, A. C., & Janikian, L., 2007. A
1022 Formação Sete Lagoas em sua área-tipo: fácies, estratigrafia e sistemas deposicionais.
1023 Revista Brasileira de Geociências, 37 (4), 1-14.
1024
- 1025 Zalán, P. V., & Silva, P. C. R., 2007. Bacia do São Francisco. Boletim de Geociências
1026 da Petrobrás, 15(2), 561-571.
1027
1028

1029 **Figure Captions**

1030

1031 *Figure 1:* Location and geology of the study area. A – São Francisco Craton, São
1032 Francisco Basin and surrounding belts (BFB=Brasilia Fold belt; Araçuaí Fold Belt). B
1033 - Simplified geological map of the Brasília Belt (after Dardenne, 2000).

1034

1035 *Figure 2:* Lithostratigraphic column of the Canastra Group (modified from Dardenne,
1036 2000). Youngest concordant age interpreted as maximum depositional age ⁽¹⁾
1037 Rodrigues et al., 2010).

1038

1039 *Figure 3:* Lithostratigraphic column of the Vazante Group (modified from Dardenne,
1040 2000). Youngest concordant age interpreted as maximum depositional age ⁽¹⁾
1041 Rodrigues et al., 2012) and Re-Os isochron interpreted as depositional age ⁽²⁾Geboy,
1042 2006; ⁽³⁾Azmy et al., 2008).

1043

1044 *Figure 4:* Seismic interpretation of the São Francisco Basin, with tunnel valleys and
1045 downwarped strata developed on the Espinhaço II Sequence.

1046

1047 *Figure 5:* Lithostratigraphic column of the Bambuí Group (modified from Dardenne,
1048 2000). Youngest concordant age interpreted as maximum depositional age ⁽¹⁾
1049 Rodrigues, 2008) and Pb-Pb isochron interpreted as depositional age ⁽²⁾Babinski et
1050 al.,2007).

1051

1052 *Figure 6:* Seismic profile in the cratonic area of the São Francisco basin showing the
1053 expression of the three shallowing-upward 2nd order sequences of the Bambuí 1st
1054 order sequence (based on Martins-Neto, 2009)

1055

1056 *Figure 7:* Stratigraphic levels of the Paracatú slate samples used for TOC and Re–Os
1057 measurements.

1058

1059 *Figure 8:* Stratigraphic levels of the Serra do Garrote slate samples used for TOC and
1060 Re–Os measurements.

1061

1062 *Figure 9:* Stratigraphic levels of the Sete Lagoas samples used for TOC and Re–Os
1063 measurements.

1064

1065 *Figure 10:* Re–Os isochron diagram for the Paracatú Formation organic-rich slates,
1066 drillhole MASW03.

1067

1068 *Figure 11:* Tentative explanation for variance of depositional TOC across the basal
1069 Sete Lagoas Formation. Core A would represent well LMR1009.

1070

1071 **Tables**

1072

1073 *Table 1:* TOC content for the Canastra, Vazante and Bambuí groups.

1074

1075 *Table 2:* Re-Os isotope data for the Paracatú and Serra do Garrote formations. *Rho is
1076 the associated error correlation at 2σ (Ludwig, 1980). §Osi is the initial ¹⁸⁷Os/¹⁸⁸Os
1077 isotope ratio calculated at 1002 Ma for the Paracatú Formation and 1300 Ma for the
1078 Serra do Garrote Formation. VZCF-6r is a repeat analysis and was not included in the

1079 regression
1080

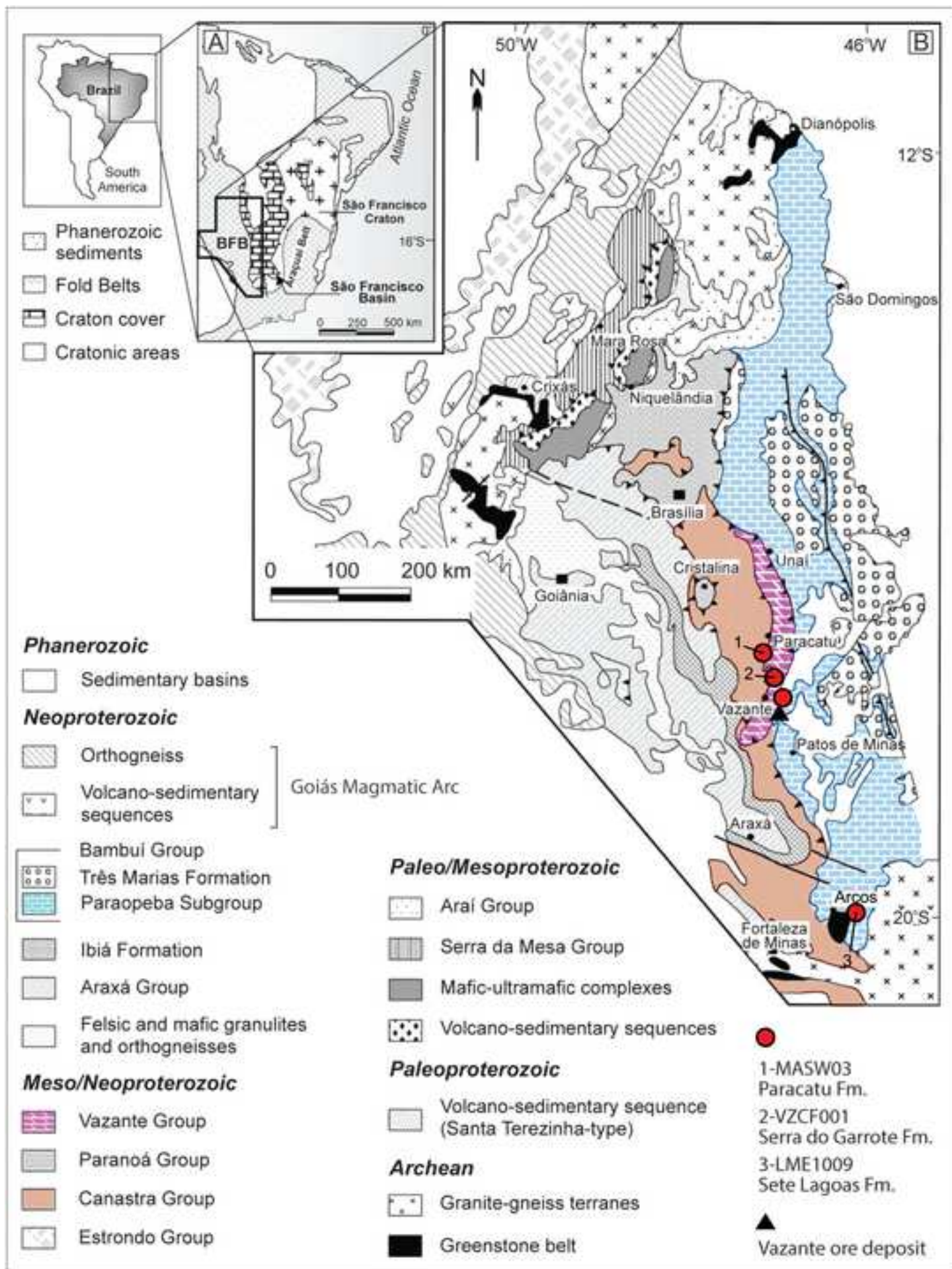
Formation	Sample	Depth [m]	TOC [wt%]
Serra do Garrote	VZCF001-1	280.23	0.85
	VZCF001-2	281.33	1.53
	VZCF001-3	281.55	0.07
	VZCF001-4	281.78	2.15
	VZCF001-5	282.00	0.87
	VZCF001-6	282.23	2.10
	VZCF001-7	285.78	0.72
	VZCF001-8	286.63	0.20
	VZCF001-9	287.78	0.93
	VZCF001-10	288.43	1.48
	VZCF001-11	288.98	0.62
	VZCF001-12	289.15	1.98
	VZCF001-13	289.60	1.50
	VZCF001-14	289.98	1.38
	VZCF001-15	292.55	1.89
Paracatú	MASW03-33	47.6	2.12
	MASW03-34	48.0	1.76
	MASW03-35	48.3	1.75
	MASW03-36	48.6	1.56
	MASW03-37	49.9	1.48
	MASW03-38	50.4	1.03
	MASW03-39	50.7	1.42
	MASW03-40	51.0	0.92
	MASW03-41	52.3	1.23
	MASW03-42	52.6	1.19
	MASW03-43	52.9	1.16
	MASW03-44	53.2	0.99
	MASW03-45	53.5	1.59
	MASW03-46	55.6	0.75
MASW03-47	55.9	1.13	
Sete Lagoas	LIMR1009-U4S15	35.85	0.08
	LIMR1009-U4S14	36.85	0.17
	LIMR1009-U4S13	37.85	0.03
	LIMR1009-U4S12	38.85	0.05
	LIMR1009-U4S11	39.85	0.02
	LIMR1009-U4S10	40.85	0.04
	LIMR1009-U4S9	41.85	0.02
	LIMR1009-U4S8	42.85	0.04
	LIMR1009-U4S7	43.85	0.10
	LIMR1009-U4S6	44.85	0.03
	LIMR1009-U4S5	45.85	0.04
	LIMR1009-U4S4	46.25	0.02
	LIMR1009-U4S3	46.65	0.01
	LIMR1009-U4S2	47.05	0.02
	LIMR1009-U4S1	47.57	0.01
	LIMR1009-U3S8	112.34	0.01
	LIMR1009-U3S7	113.34	0.01
	LIMR1009-U3S6	114.34	0.02
	LIMR1009-U3S5	115.34	0.08
	LIMR1009-U3S4	116.34	0.01
	LIMR1009-U3S3	116.74	0.04
	LIMR1009-U3S2	117.14	0.03
	LIMR1009-U3S1	117.54	0.02
	LIMR1009-U2S15	145.75	0.00
	LIMR1009-U2S14	146.75	0.00
	LIMR1009-U2S13	147.75	0.00
	LIMR1009-U2S12	148.75	0.02
	LIMR1009-U2S11	149.75	0.00
	LIMR1009-U2S10	150.75	0.02
	LIMR1009-U2S9	151.75	0.08
LIMR1009-U2S8	152.75	0.00	

LIMR1009-U2S7	153.75	0.01
LIMR1009-U2S6	154.75	0.01
LIMR1009-U2S5	155.75	0.00
LIMR1009-U2S4	156.15	0.01
LIMR1009-U2S3	156.55	0.06
LIMR1009-U2S2	156.95	0.02
LIMR1009-U2S1	157.35	0.13
LIMR1009-U1S1	158.15	0.32
LIMR1009-U1S2	158.55	0.22
LIMR1009-U1S3	158.95	0.24
LIMR1009-U1S4	159.35	0.24
LIMR1009-U1S5	159.75	0.22
LIMR1009-U1S6	160.75	0.06
LIMR1009-U1S7	161.75	0.36
LIMR1009-U1S8	162.75	0.14
LIMR1009-U1S9	163.75	0.49
LIMR1009-U1S10	164.75	0.33

Table

Sample	Re (ppb)	±	Os	±	$^{187}\text{Re}/^{188}\text{Os}$	±	$^{187}\text{Os}/^{188}\text{Os}$	±	Rho*	Osi [§]
Paracatú										
MASW03-36	0.30	0.001	64.8	1.2	24.2	0.3	0.667	0.038	0.705	0.260
MASW03-38	0.36	0.001	52.7	1.0	36.1	0.7	0.847	0.030	0.705	0.239
MASW03-40	4.11	0.013	296.5	2.1	79.6	0.8	1.593	0.040	0.656	0.253
MASW03-42	1.31	0.004	175.1	1.0	39.8	0.6	0.934	0.030	0.654	0.264
Serra do Garrote										
VZCF-6	18.7	0.06	507.2	5.2	317.9	2.8	6.167	0.070	0.656	-0.793
VZCF-6r	18.9	0.06	515.7	9.3	314.3	6.4	6.136	0.174	0.698	-0.746
VZCF-11	9.2	0.03	260.2	2.5	269.9	2.4	4.654	0.053	0.657	-1.255
VZCF-13	28.3	0.09	584.6	7.0	601.2	5.2	12.207	0.139	0.656	-0.956
VZCF-3B	4.0	0.01	136.8	2.2	205.1	4.2	3.628	0.103	0.699	-0.862

Figure
[Click here to download high resolution image](#)



Figure

[Click here to download high resolution image](#)

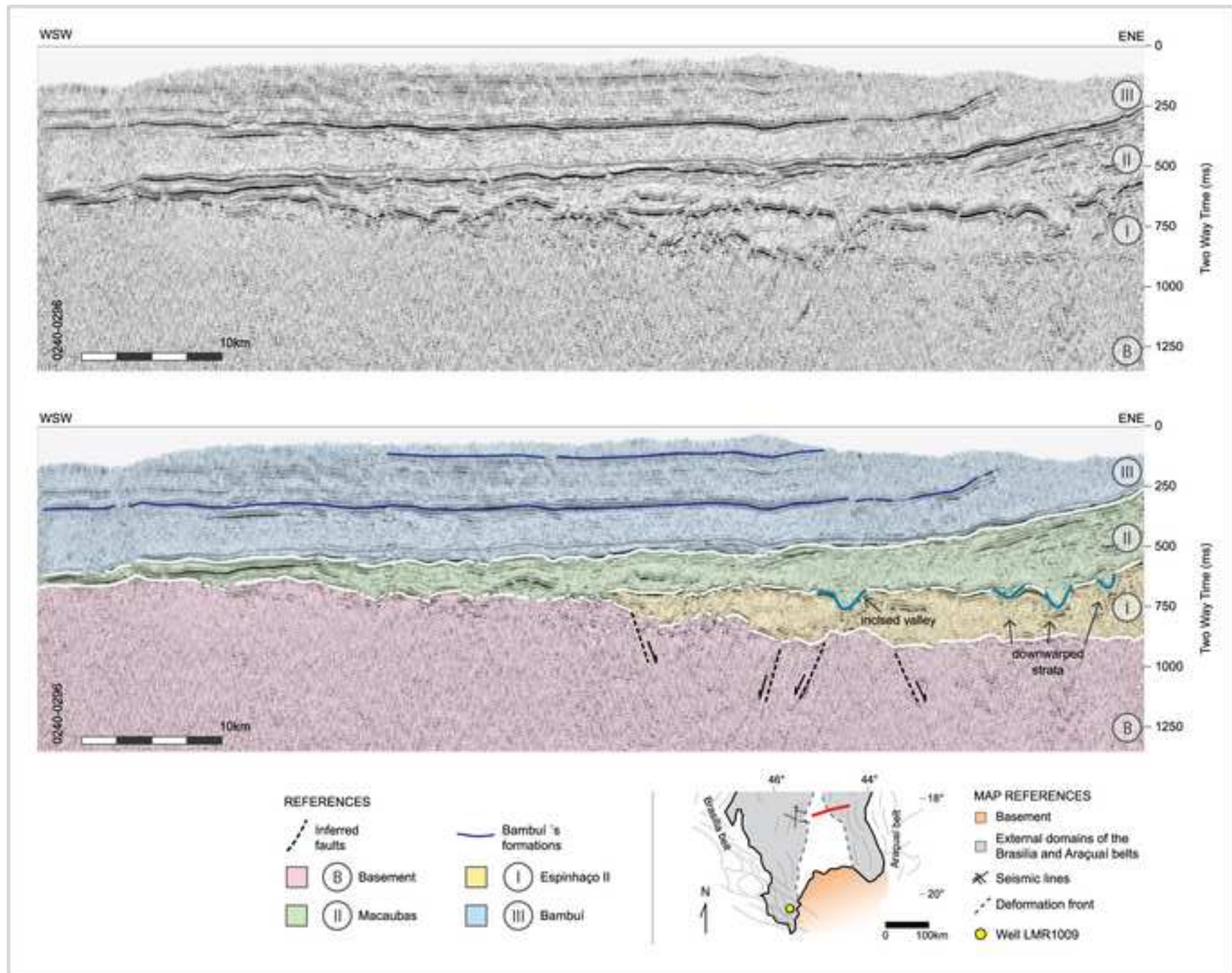
Group	Formation	Member	Lithology	Youngest concordant age (Ma)
CANASTRA	Chapada dos Pilões	Hidrelétrica da Batalha	Quartzite and phyllite interbedded	1070 ⁽¹⁾
		Serra da Urucânia	Sandy metarhythmite and intercalation of quartzite	
	Paracatu	Serra da Antia	Sericite phyllite and intercalation of carbonaceous phyllite and quartzite	1040 ⁽¹⁾
		Morro do Ouro	Carbonaceous phyllite and intercalations of quartzite and sericite phyllite	
	Serra do Landim		Calciferous phyllite	1079±45 ⁽¹⁾

Figure

[Click here to download high resolution image](#)

Group	Formation	Lithology	Youngest concordant age (Ma)	Depositional age (Ma)	
VAZANTE	Lapa	Carbonaceous phyllite, carbonatic metasilstone quartzites, conglomerate and slate	1084±14 ⁽¹⁾	1000-1100 ⁽³⁾	
	Morro do Calcário	Dolomitic biostromes and bioherms, breccia, dolonudite, oolitic dolarenite and oncolites	1137±8 ⁽¹⁾		
	Sierra do Poço Verde	Limestones with stromatolitic mats and mud crack			1128±47 ⁽²⁾
		Slate with intercalations of dolomite			
		Dolomite with stromatolitic mats and bird's eyes			
	Sierra do Garrote	Dolomite with layers of breccias and dolarenite			
		Carbonaceous pyrite-bearing slate with rare fine quartzite intercalations	1296±13 ⁽¹⁾	1353±69 ⁽²⁾	
	Lagamar	Stromatolitic bioherms interdigitated with carbonate-bearing metasilstone and slate. Intraformational dolomitic breccia.			
		Conglomerate, quartzite, metasilstone and slate			
	Rocinha	Phosphoarenite rich in intraclasts and pellet			
Slate, with pyrite and phosphorite		935±14 ⁽¹⁾			
Rhythmic package of slate and metasilstone					
Santo Antônio do Bonito/Ruído	Quartzite, intercalated with slate. Diamictite	997±29 ⁽¹⁾			

Figure
[Click here to download high resolution image](#)



Figure

[Click here to download high resolution image](#)

Group	Formation	Lithology	Youngest concordant age (Ma)	Depositional age (Ma)	
BAMBUÍ	Paracopeba Subgroup	Três Marias	Fine arkose and immature siltstone	616 ⁽¹⁾	
		Serra da Saudade	Slate, mudstone, argillaceous siltstone and rare lenses of limestone	612 ⁽¹⁾	
		Lagoa do Jacaré	Calciferous siltstone, limestone, argillaceous layers and lenses of oolitic limestone		
		Serra da Santa Helena	Slate, laminated siltstone and rare thin layers of sandstone	650 ⁽¹⁾	
		Sete Lagoas	Crystalline limestone, pelitic rhythmite, lime mudstone, black crystalline limestone, marble	610 ⁽¹⁾	740±22 ⁽²⁾

Figure

[Click here to download high resolution image](#)

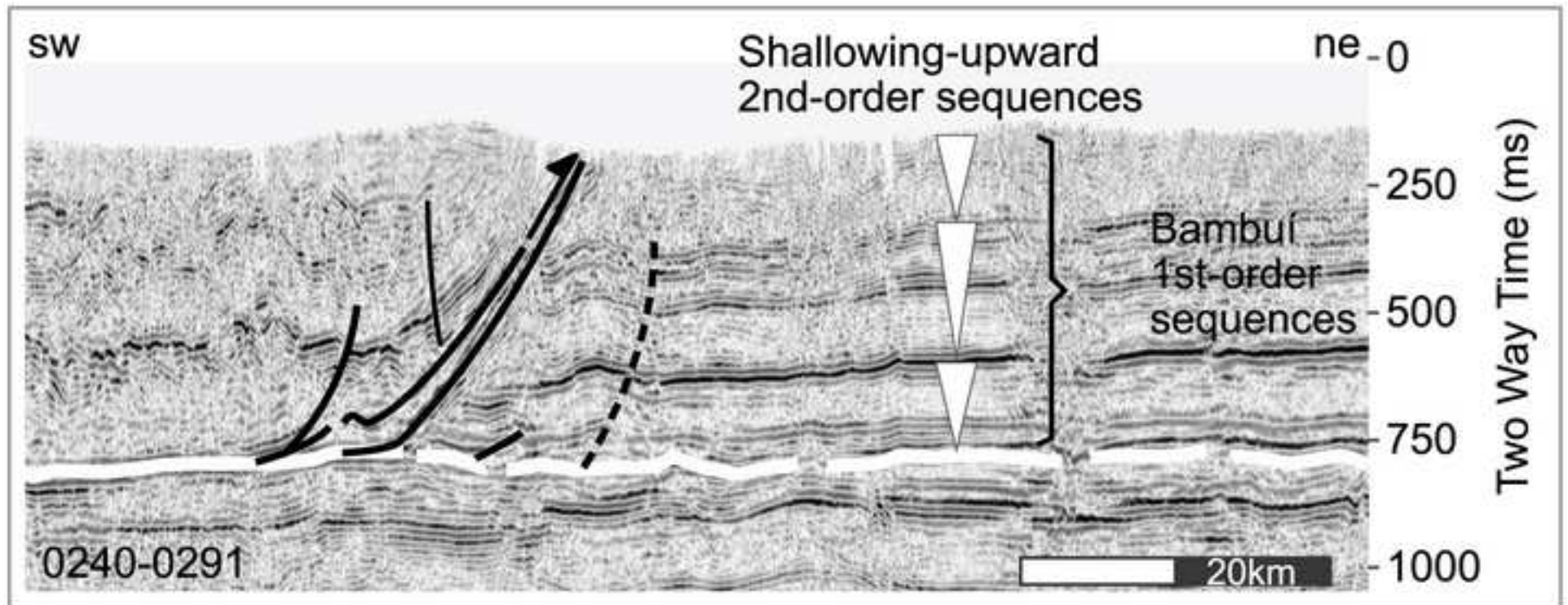
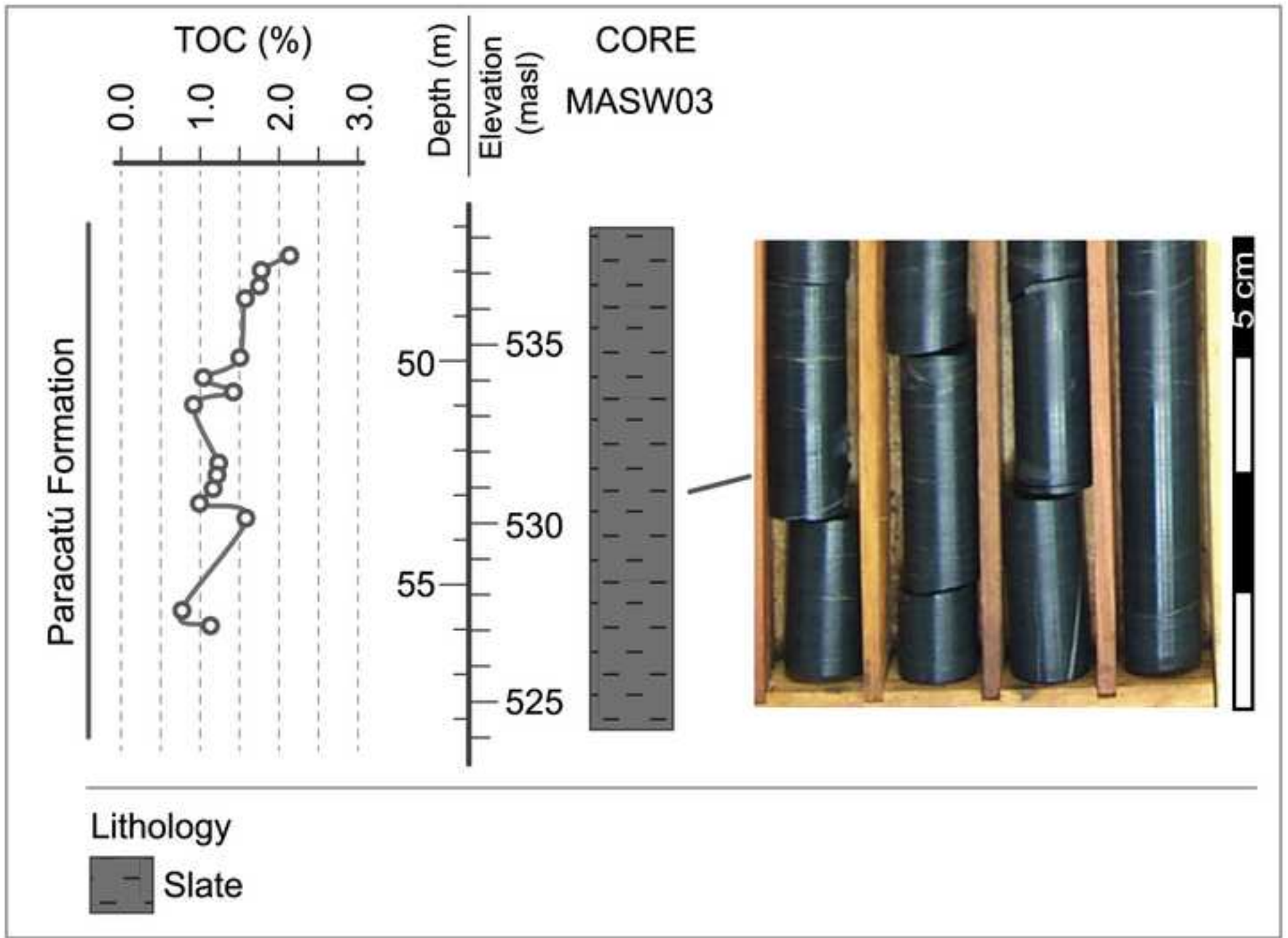
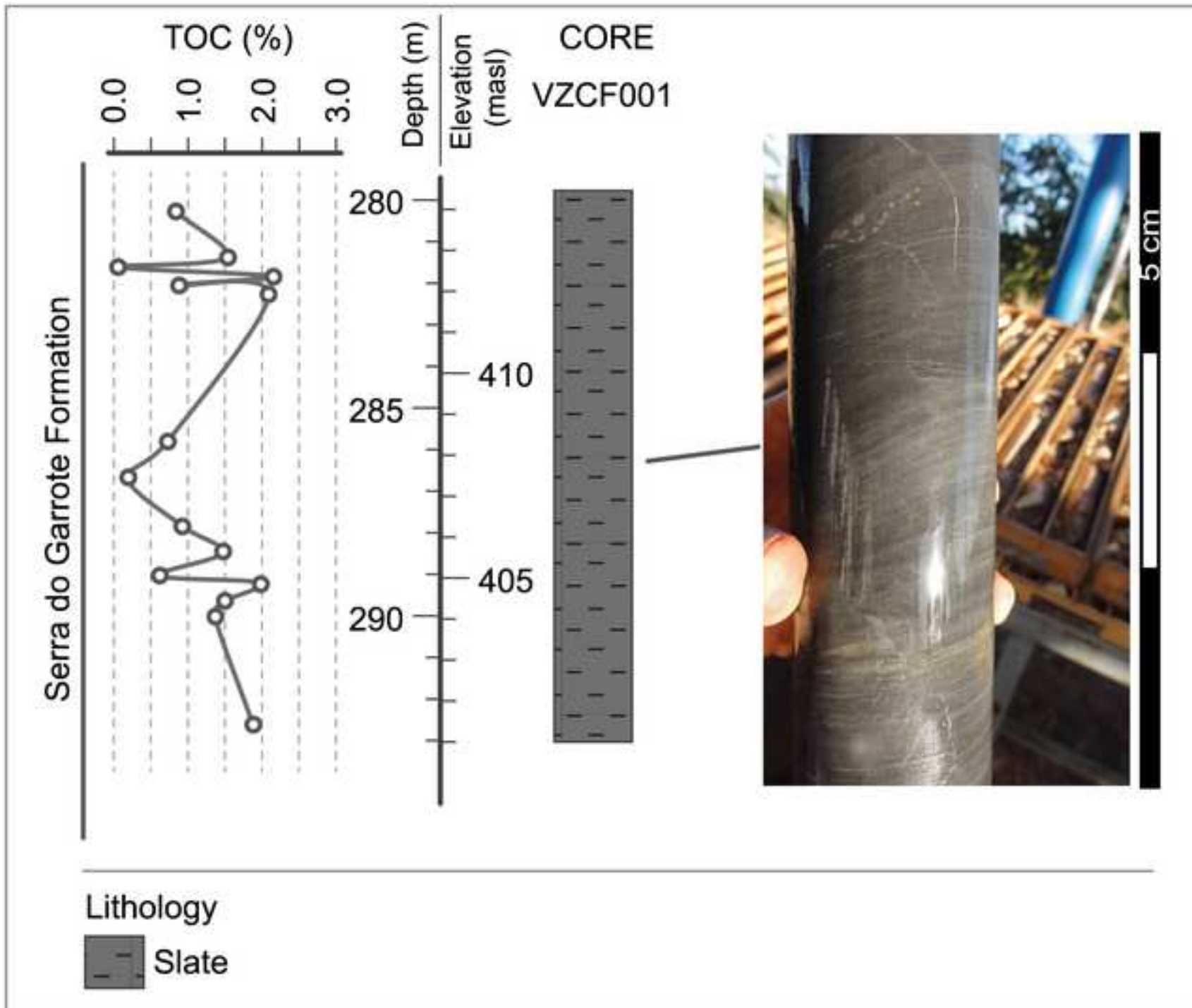


Figure
[Click here to download high resolution image](#)



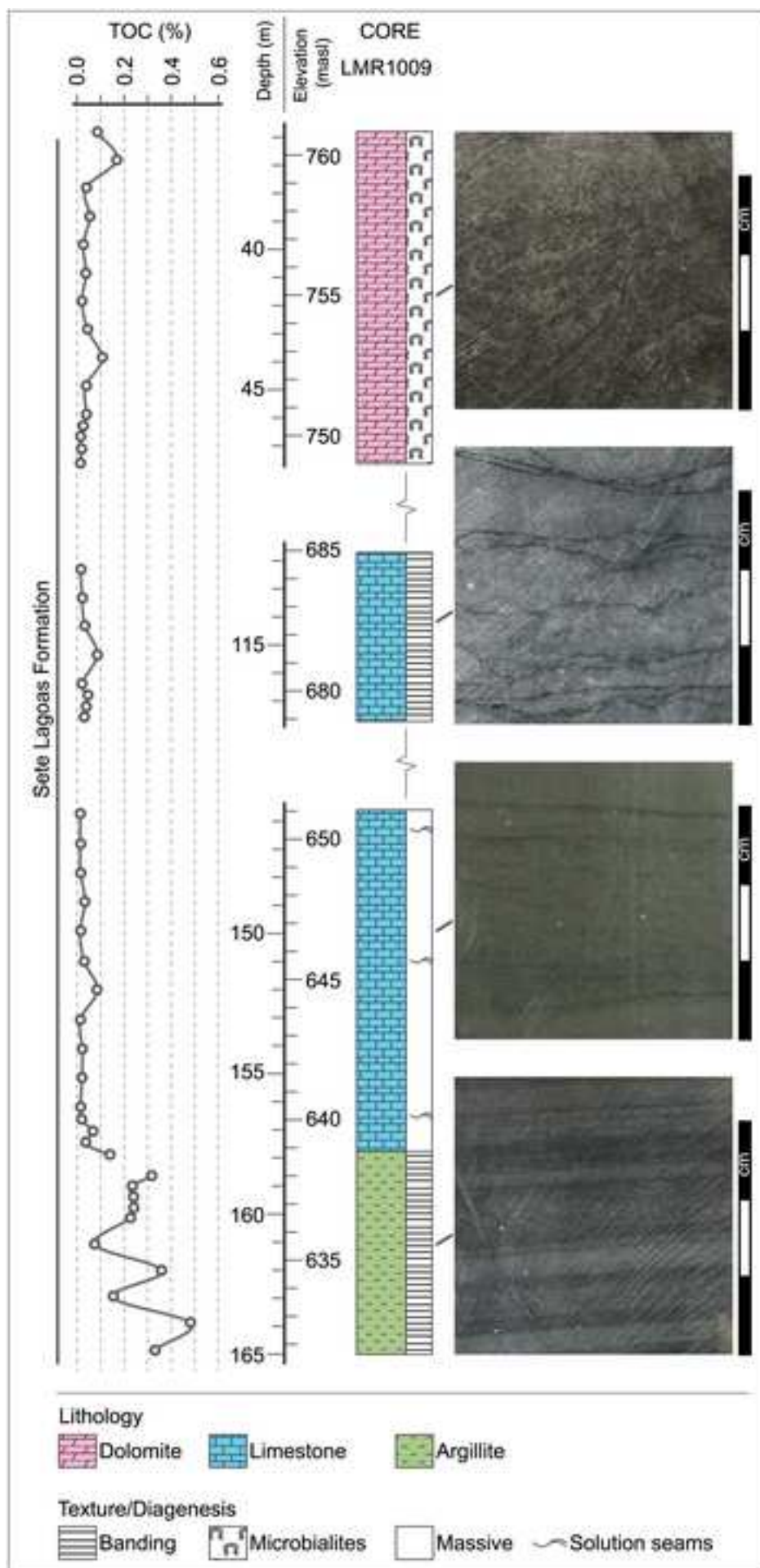
Figure

[Click here to download high resolution image](#)



Figure

[Click here to download high resolution image](#)



Figure

[Click here to download high resolution image](#)

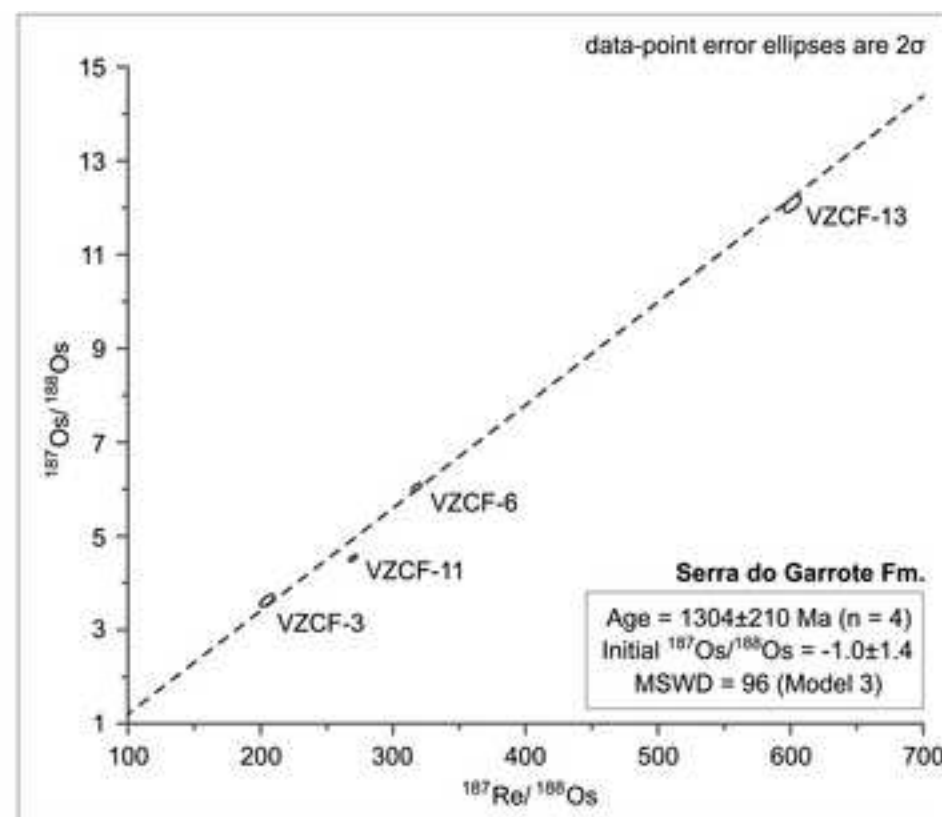
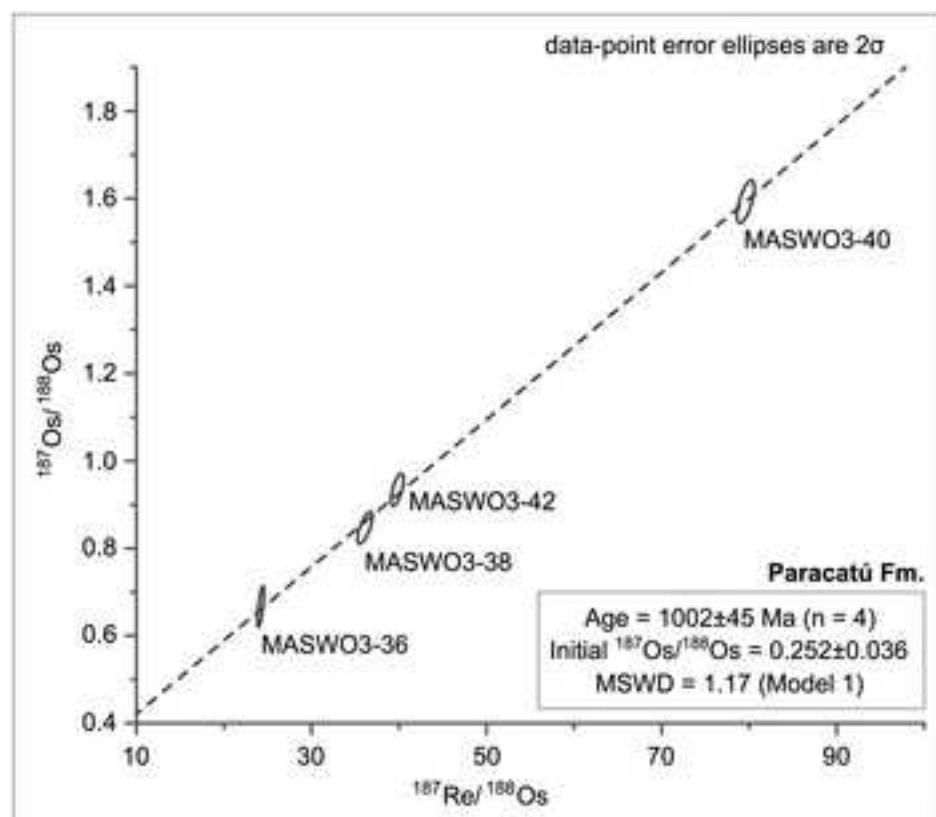


Figure
[Click here to download high resolution image](#)

